Low pile-up pT(W) measurement from ATLAS

Zhibo Wu

On behalf of ATLAS

30/11/2023

Conference note: ATLAS-CONF-2023-028

The motivation the p_T^W measurement

Reduce the p_T^W modelling uncertainty in the m_W measurement.

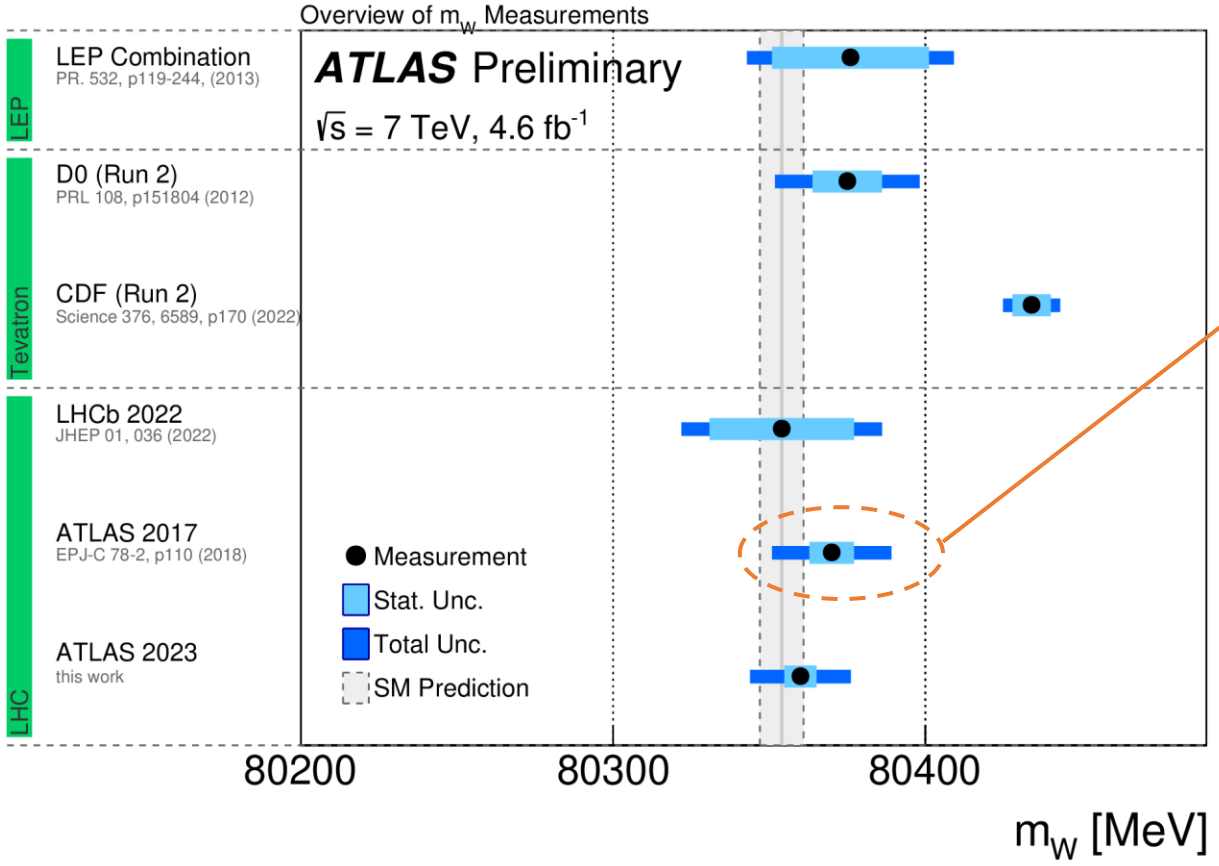

- ATLAS 7 TeV m_W analysis:

6 MeV p_T^W modelling uncertainty dominated by the p_T^Z-> p_T^W extrapolation uncertainties.

- Solution:

-> Direct p_T^W measurement.

Targeted p_T^W precision:

- A granularity of 6~7 GeV.
- 1~2% uncertainty in the low values of p_T^W where the fixed-order perturbative prediction fails.

Event topology: leptonic decay of W/Z

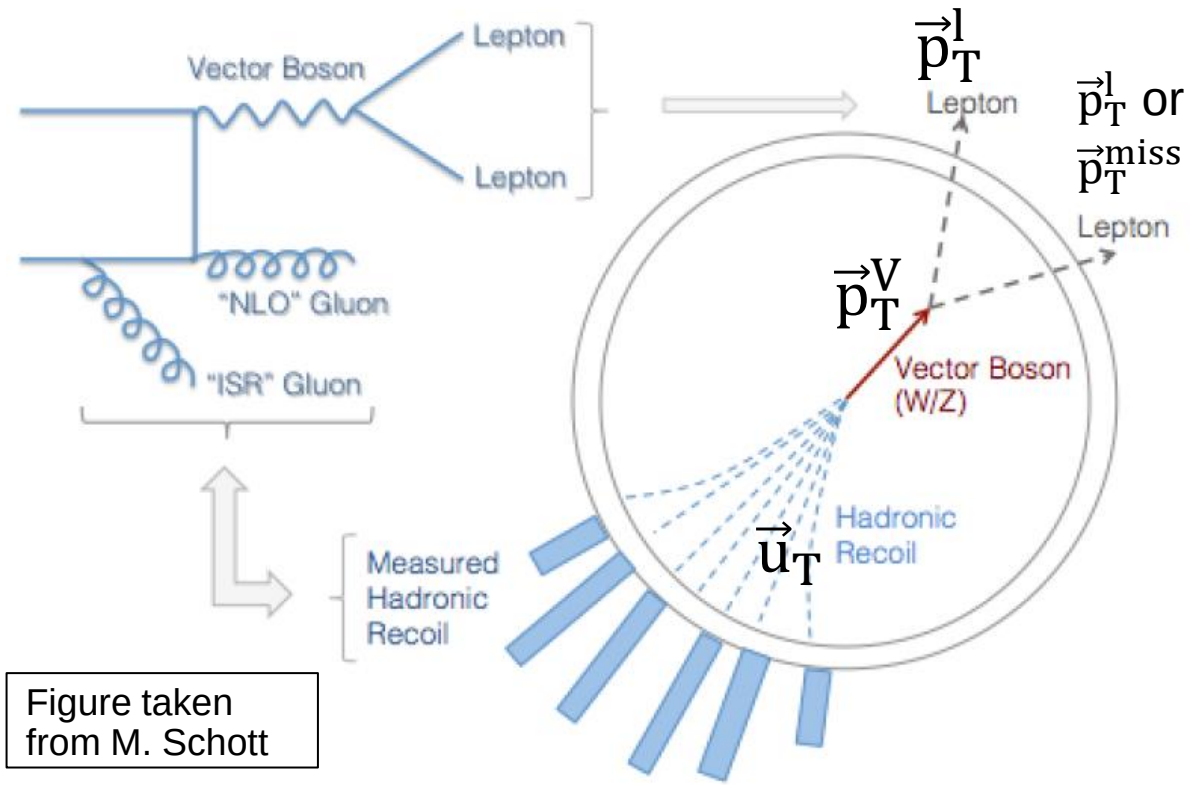

Figure taken from M. Schott

In W events:

$$m_T = \sqrt{2 p_T^l p_T^{miss} \left(1 - \cos\left(\phi_l - \phi_{p_T^{miss}}\right)\right)}$$

$\vec{p}_T^{\,miss} = -\left(\vec{p}_T^{\,l} + \vec{u}_T\right)$ for the neutrino

- Only **two objects** to measure:

(1) The charged lepton

(2) Hadronic recoil $\vec{u}_T = \Sigma \vec{p}_T^{\,ISR\ q,g} = -\vec{p}_T^{\,V}$

W events: u_T -> p_T^W

Z events: p_T^{ll} -> p_T^Z or u_T -> p_T^Z

- Detector calibrations are needed for lepton and recoil.
- Detector resolution of u_T is affected by underlying event and pile-up.

Lower pile-up in the dataset

-> More precise measurement of p_T^W

ATLAS Run 2 low pile-up data

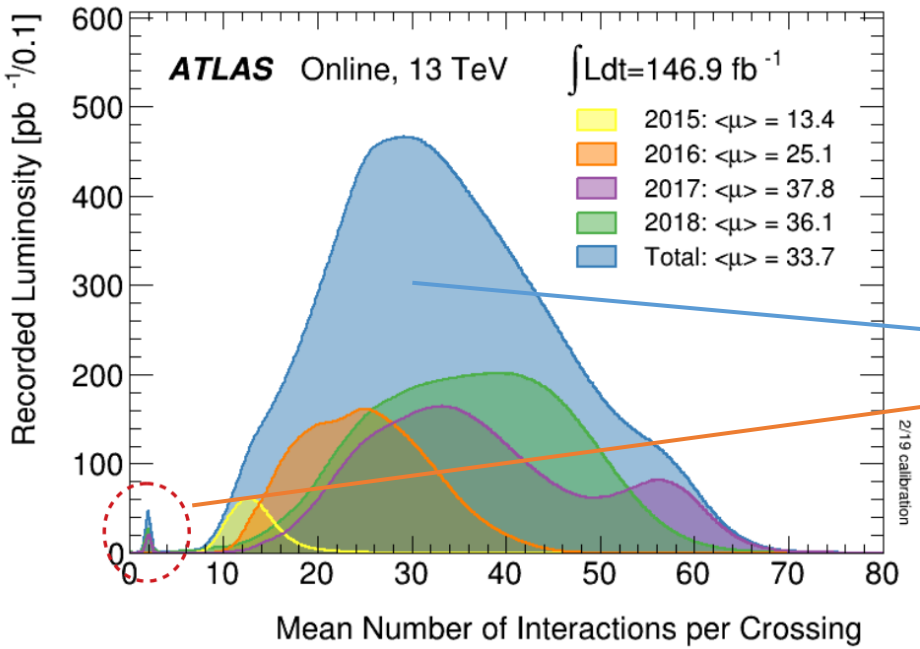

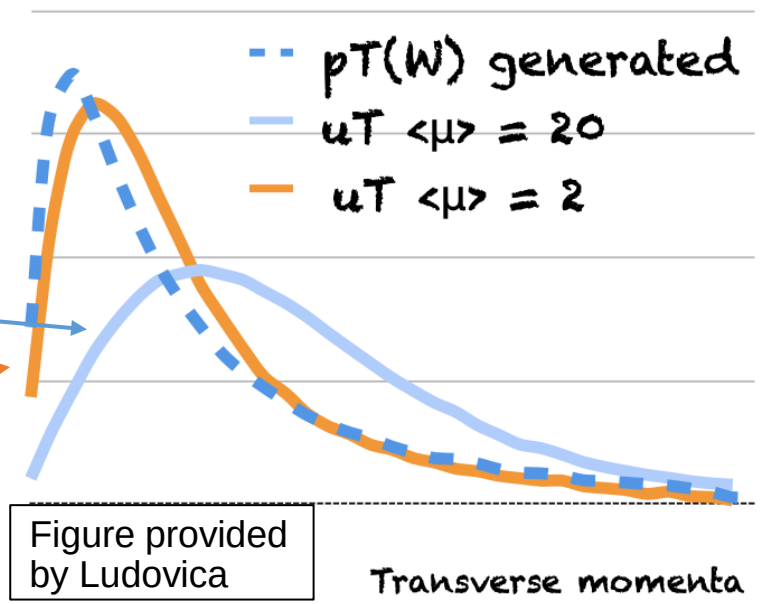

Figure provided by Ludovica

Probes of perturbative and non-perturbative QCD in W events, as well as in Z events at 5.02 TeV.

	2017, $\sqrt{s}$=5.02 TeV	2017+2018, $\sqrt{s}$=13 TeV
Luminosity (pb^{-1})	255	338
W^+ events after selection	888K	2.45M
W^- events after selection	562K	1.91M
Total W events after selection	1.45M	4.36M
Total Z events after selection	122K	379K

Event display of the low pile-up data

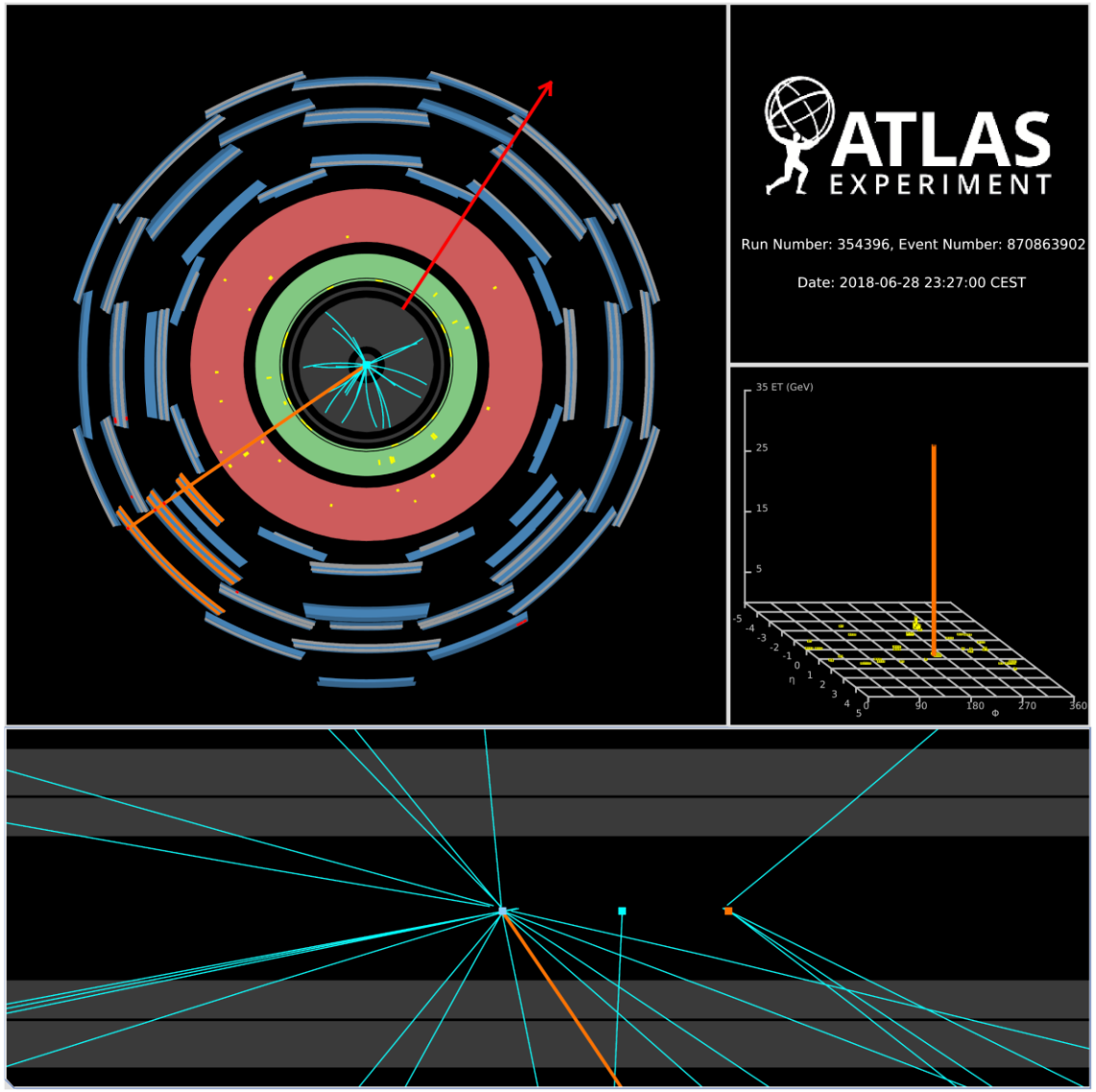

The event display of a W^- boson candidate at 13 TeV.

- Orange line: muon
- Red arrow: missing transverse momentum

Event kinematics:

- p_T^{μ}=35 GeV
- Reconstructed p_T^{W} = 16 GeV
- m_T=77 GeV
- p_T^{miss}=49 GeV.

MC samples and event selection

MC simulations were produced to match the low pile-up condition in data.

- W & Z production: Powheg+Pythia8 AZNLO, CT10 PDF
- Top-related background: Powheg+Pythia8
- Di-boson background: Sherpa
- Minimum-bias events: Pythia8 A3 tune with NNPDF2.3LO

Cut	Description
One charged lepton	Exactly one electron or muon
Lepton trigger matched	• 1 electron, $E_T > 15\ \mathrm{GeV}$, loose ID. • Or 1 muon, $E_T > 14\ \mathrm{GeV}$.
Isolation	Ptcone20 / Min(p_T^l, 50GeV) < 0.1
Kinematics	$p_T^l > 25\ \mathrm{GeV}$
	$p_T^{miss} > 25\ \mathrm{GeV}$
	$m_T > 50\ \mathrm{GeV}$

Analysis cuts for W signal selection

Physics corrections

- Vertex z-position correction.
- Vertex efficiency correction: Correct the efficiency of primary vertex association for W→lν events in the simulations.
- QED FSR: Powheg+Pythia8 interfaced to PHOTOS++.
- W, Z polarization: Ai's are calculated by DYTURBO at fixed-order NNLO using CT10NNLO PDF.
- $\mathrm{p_T^V}$ modelling correction: The underling $\mathrm{p_T^V}$ spectra predicted by Powheg+Pythia8 are reweighted by functions of $\mathrm{p_T^V}$ to optimize the reco-level data/MC agreement.

➢8 different $\mathrm{p_T^V}$ reweighting functions are determined individually for $\mathrm{W^{\pm}}$, Z ($\mathrm{u_T}$) and Z ($\mathrm{p_T^{\mathit{ll}}}$) at two center-of-mass energies.

Detector calibration: lepton

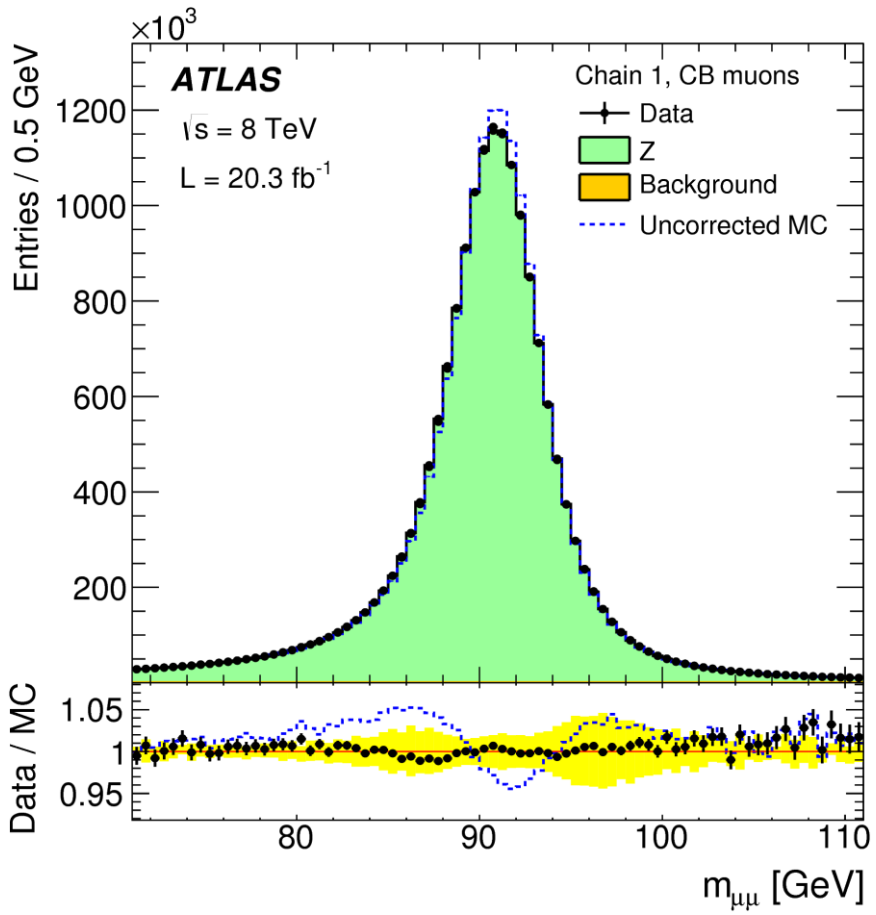

The lepton momentum in the simulation is corrected to reproduce the resonance of Z-boson in data.

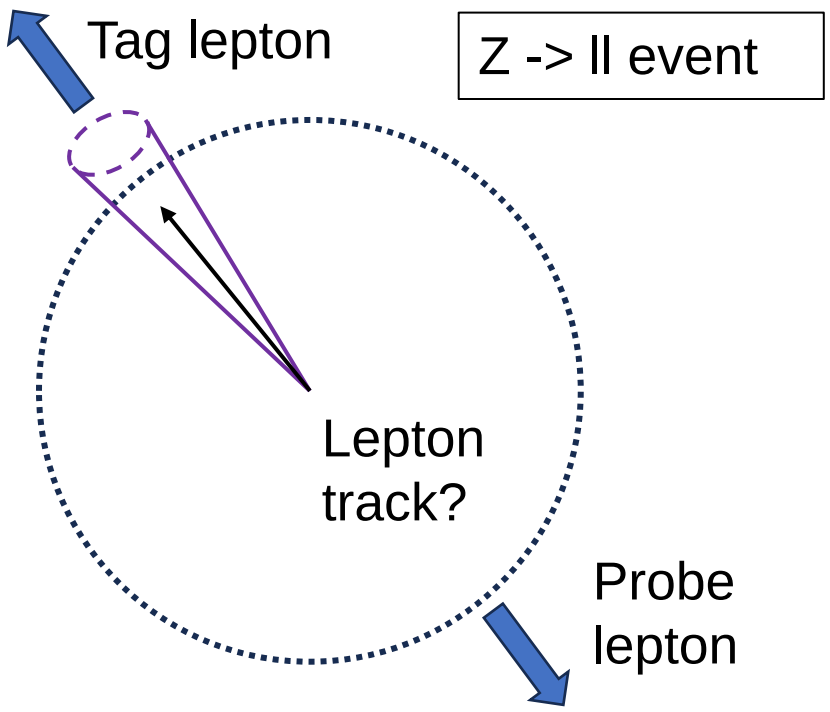

Efficiency measured in Z->ll events with tag & probe:

- Tighten the selection on one of the leptons (tag) to ensure the signal purity.
- Measure the selection efficiency on the second, unbiased lepton (probe).

Detector calibration: hadronic recoil

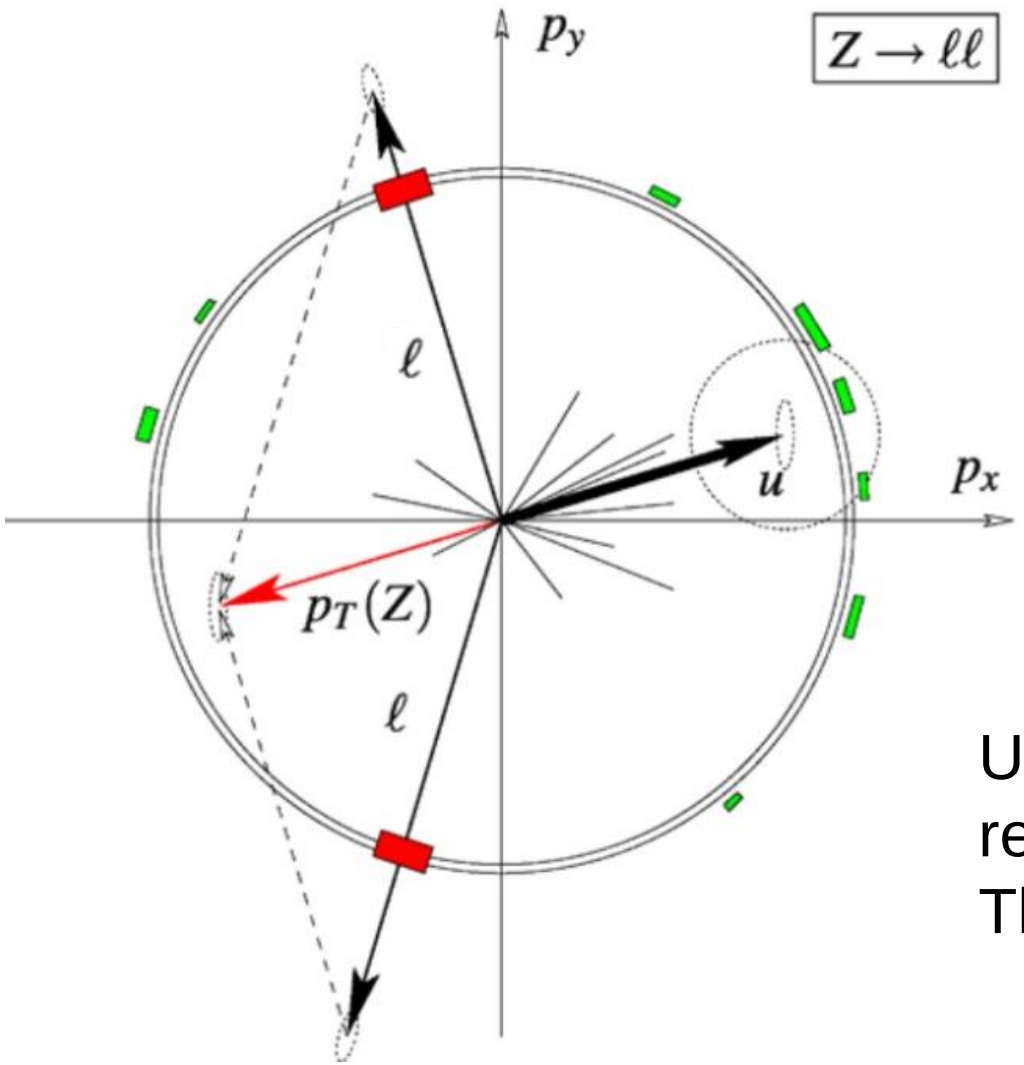

- In Z->ll events, the transverse momentum of the di-lepton pair ($\mathrm{p_T^{ll}}$) is well-measured.
- $\mathrm{p_T^{ll}}$ corresponds to the transverse momentum of Z-boson ($\mathrm{p_T^Z} = \mathrm{p_T^{ll}}$).

Use the $\mathrm{p_T^{ll}}$ constraint to calibrate the response and resolution of $\mathrm{u_T}$ in Z->ll events. Then extrapolate the results to W events.

Hadronic recoil calibration and correction

The calibration is obtained as a function of $\sum \overline{E}_T$ and p_T^V: $(\sum \overline{E}_T = \sum E_T - u_T)$

- $\sum \overline{E}_T$ modelling
- Azimuthal angle corrections
- Response and resolution corrections

Uncertainty sources:

- $\sum \overline{E}_T$ reweighting uncertainty.
- Response and resolution uncertainties.
- Since the Z-based calibration is applied to W, the uncertainties due to this extrapolation are taken into account.

13 TeV Z->μμ events

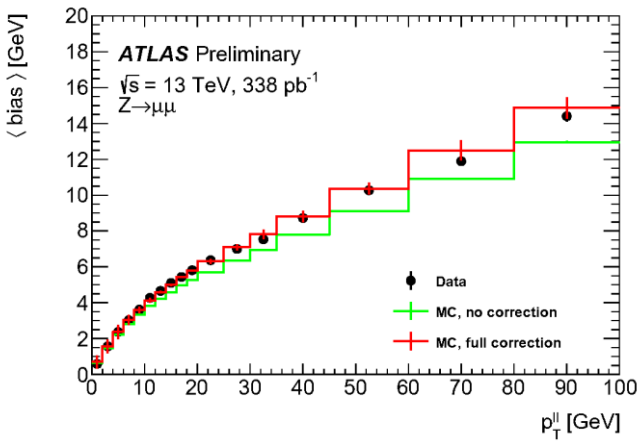

Mean value for bias $b = u_{\parallel} + p_T^{ll}$.

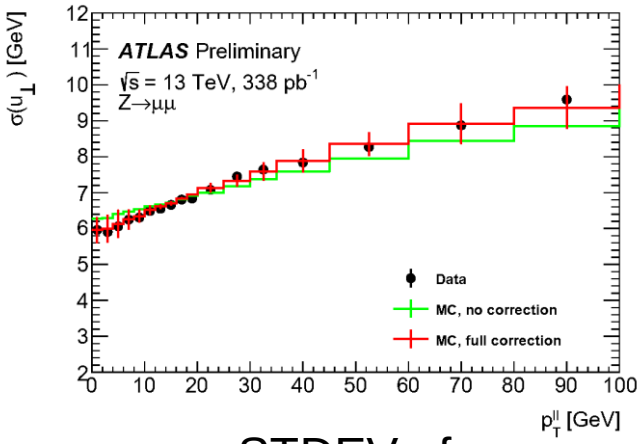

STDEV of $u_{\perp}$.

Multijet estimation

- MJ sources: heavy quark decay, in-flight pion decay, photon conversion.

- Data-driven methods are applied to both W and Z:

(a) Determination of yield.

(b) Derivation of MJ shape.

➢The MJ fraction is below 0.1% for all Z channels.

➢ MJ fraction 0.6%~2.9% for W at 13 TeV, 0.1%~0.8% for W at 5.02 TeV

Reconstructed level control plots

u_T in 5.02 TeV
$W^- \rightarrow ev$ channel

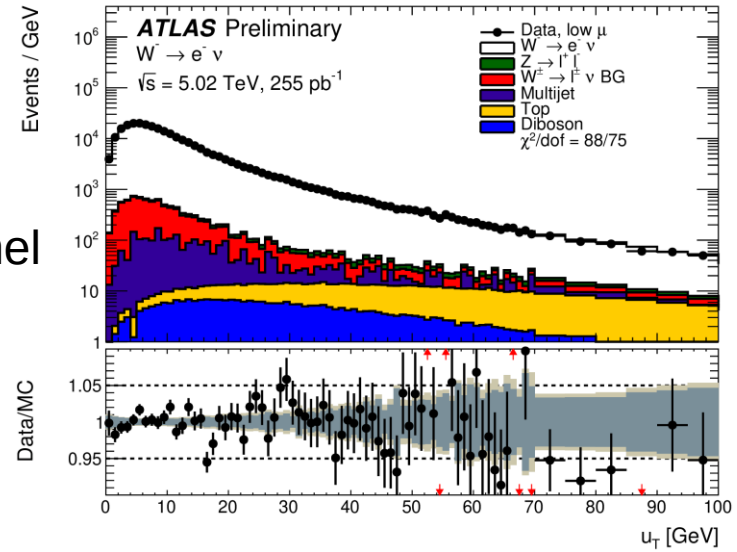

p_T^{ll} in 5.02 TeV
$Z \rightarrow ee$ channel

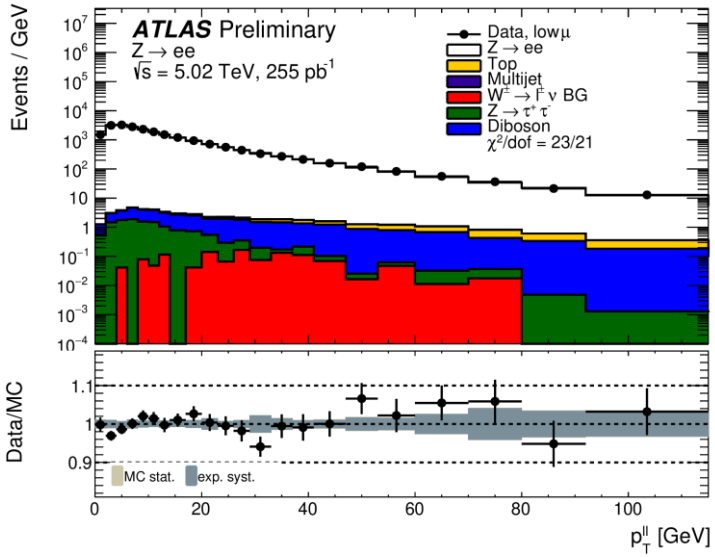

u_T in 13 TeV
$W^- \rightarrow ev$ channel

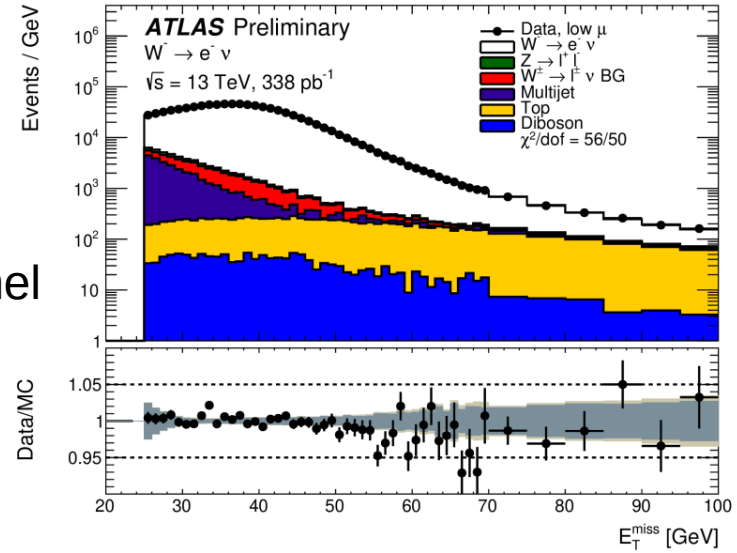

p_T^{ll} in 13 TeV
$Z \rightarrow ee$ channel

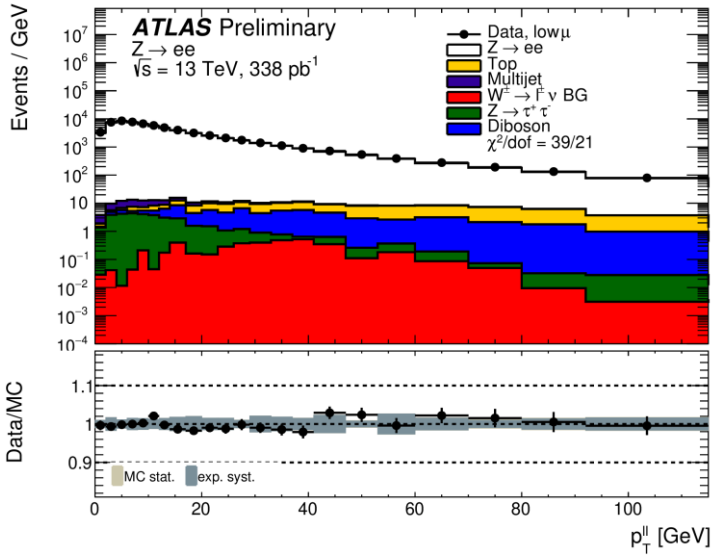

Unfolding

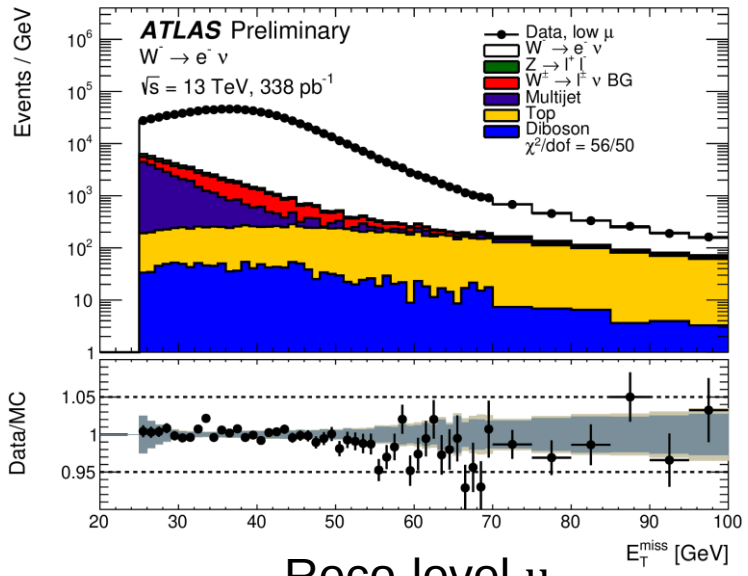

Reco-level u_T

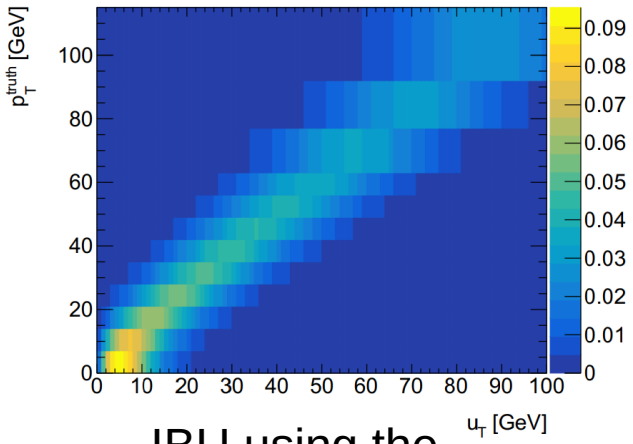

IBU using the migration matrix

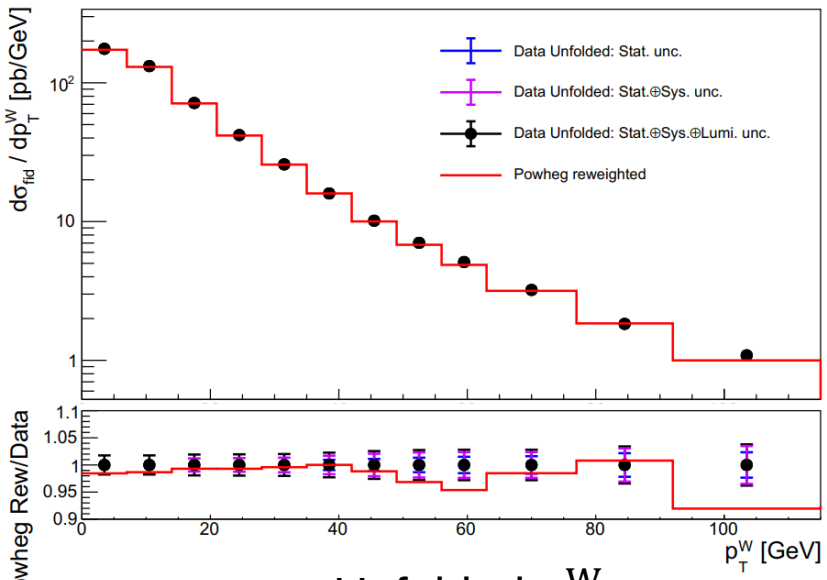

Unfolded p_T^W

- Iterative Bayesian unfolding for p_T^W: $\vec{u}_T = \Sigma \vec{p}_T^{\,ISR\ q,g} = -\vec{p}_T^{\,V}$
- p_T^Z spectrum can be obtained by unfolding u_T and p_T^{ll}.

-> Compatibility test of the unfolding

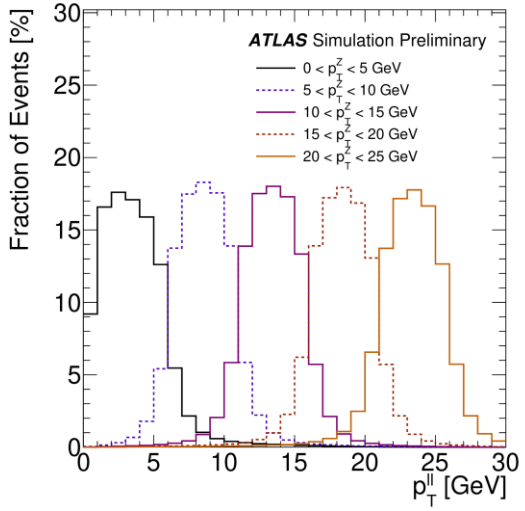

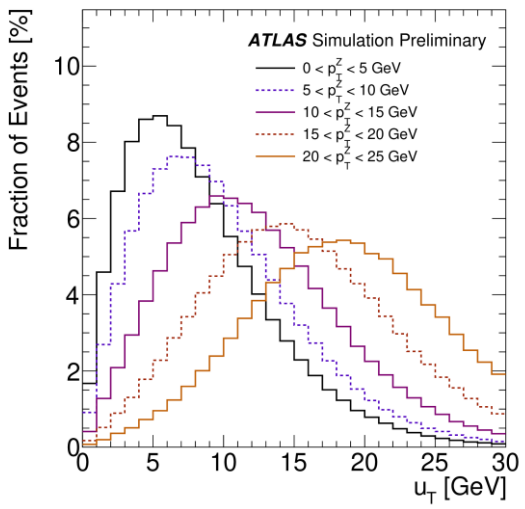

Unfolding

Iterative Bayesian Unfolding:

- u_T -> p_T^W: 9 (25) iterations with 7 GeV bin width in the low p_T^W region for W channels at 5.02 (13) TeV.
- p_T^{ll} -> p_T^Z: 2 iterations with 7 GeV bin width at low p_T^Z for Z.

Fiducial volume:

- p_T^l > 25 GeV, $|\eta_l|$<2.5
- W events: p_T^ν > 25 GeV and m_T^W > 50 GeV
- Z events: 66 < m_{ll} < 116 GeV

The variations & non-closures of the data-driven p_T^V modelling correction are accounted for as unfolding bias uncertainties.

Combination and χ^2

- At each center-of-mass energy, the electron and muon channels are combined for each charge of the boson.
- Statistical procedure: BLUE prescription with 4 iterations.

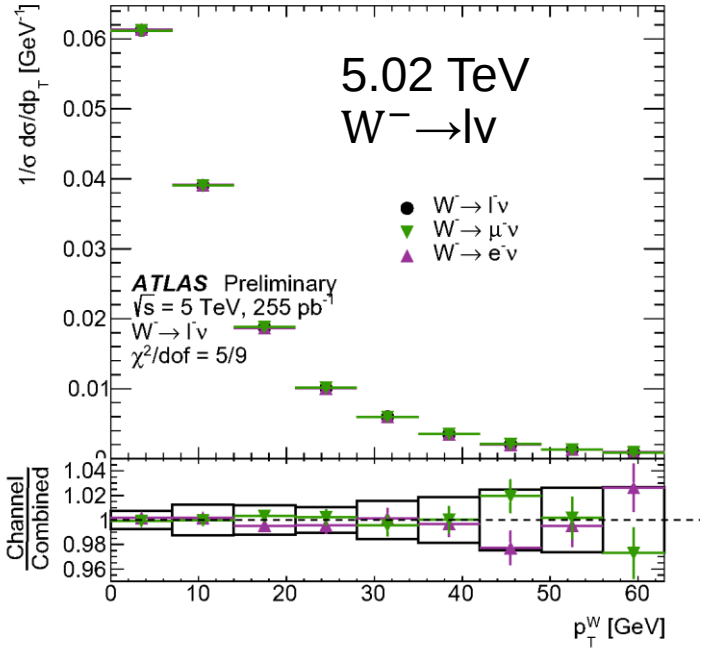

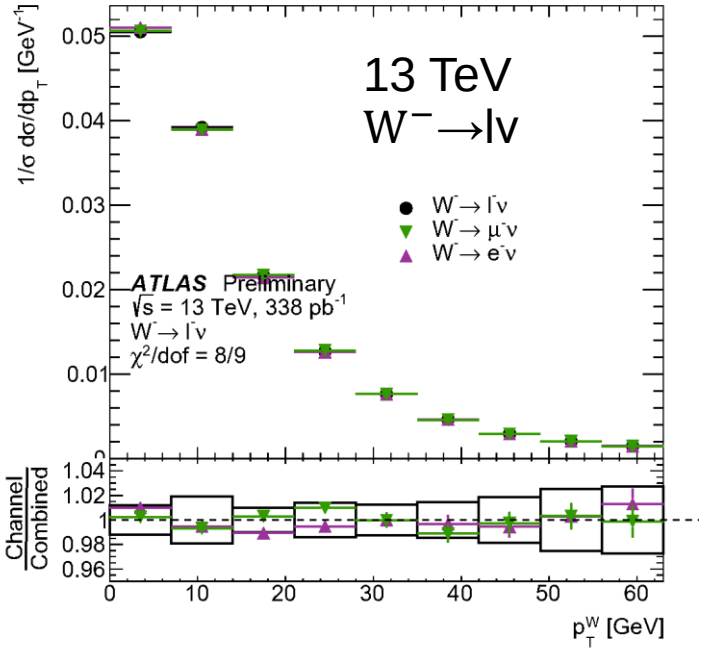

Channel	χ^2/dof
5.02 TeV	
$W^- \to \ell^- \nu$	14.6/15
$W^+ \to \ell^+ \nu$	14.5/15
$W \to \ell\nu$	12.1/15
$Z \to \ell\ell$	13.7/26
$W^+ \to \ell^+\nu$ / $W^- \to \ell^-\nu$	13.0/15
$W \to \ell\nu / Z \to \ell\ell$	16.3/15
13 TeV	
$W^- \to \ell^- \nu$	16.0/17
$W^+ \to \ell^+ \nu$	17.6/17
$W \to \ell\nu$	22.1/17
$Z \to \ell\ell$	21.4/27
$W^+ \to \ell^+\nu$ / $W^- \to \ell^-\nu$	11.3/17
$W \to \ell\nu / Z \to \ell\ell$	17.1/17
Ratio 13 TeV/5.02 TeV	
$W^- \to \ell^- \nu$	11.5/15
$W^+ \to \ell^+ \nu$	9.3/15
$W \to \ell\nu$	7.3/15
$Z \to \ell\ell$	14.2/25

Good compatibility is found between electron and muon channels.

Uncertainty break-down for p_T^W

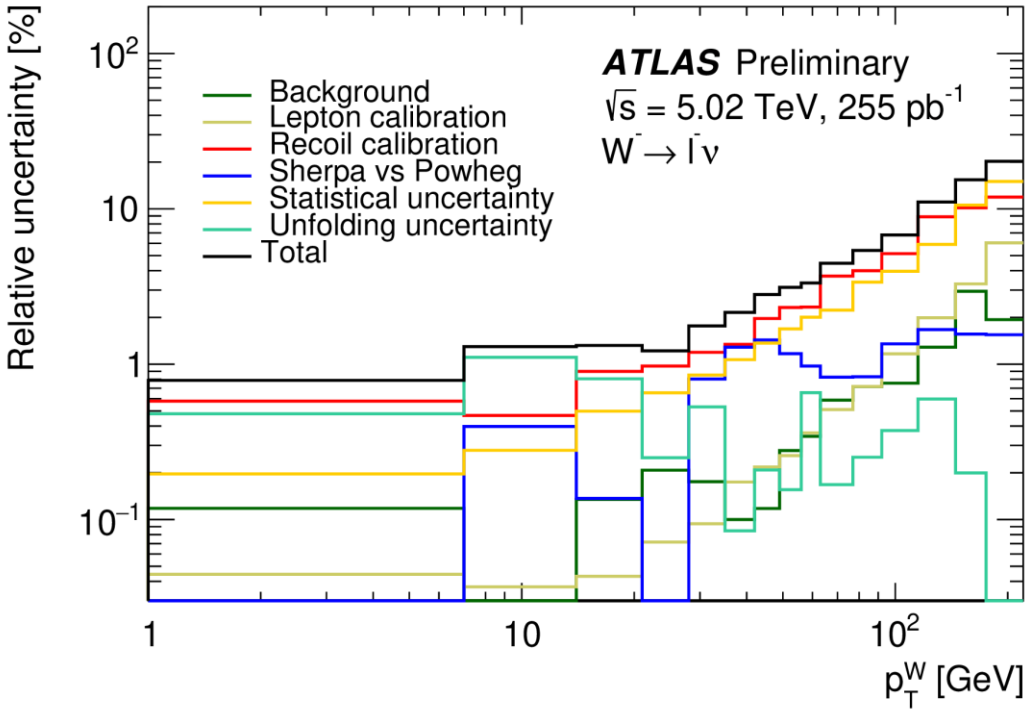

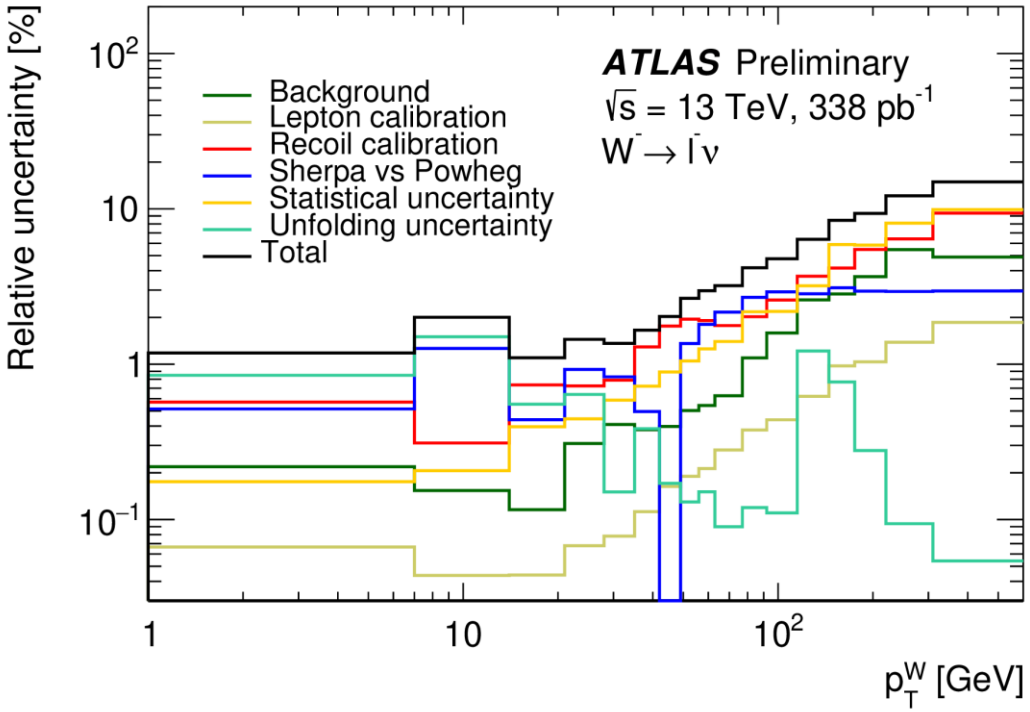

Break-down of p_T^W uncertainty for the combined $W^- \rightarrow l\nu$ measurements at 5.02 TeV (left) and at 13 TeV (right).

Leading systematic sources in the low p_T region:

- Unfolding uncertainties
- Recoil calibration systematics.
- “Sherpa vs Powheg” generator systematics

Total uncertainty achieves the goal: **1-2%** in the low p_T with a granularity of **7 GeV**.

Uncertainty break-down for $p_T^Z(p_T^{ll})$

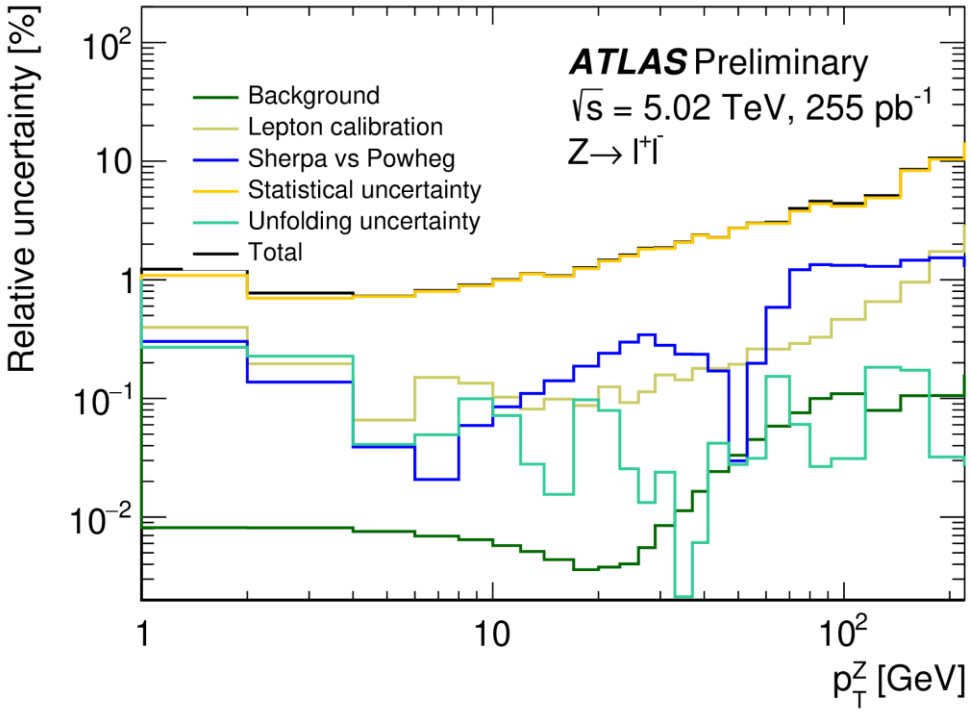

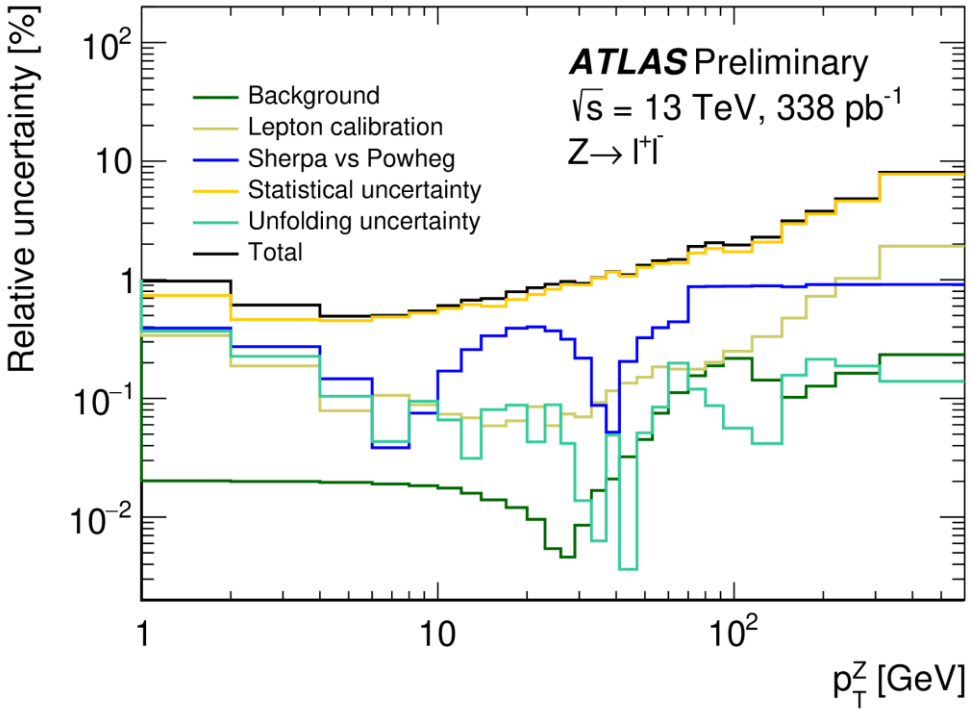

Break-down of p_T^Z uncertainty for the combined Z→ll measurements at 5.02 TeV (left) and at 13 TeV (right).

- Dominated by statistical uncertainty.

p_T^W differential cross-section: 5.02 TeV

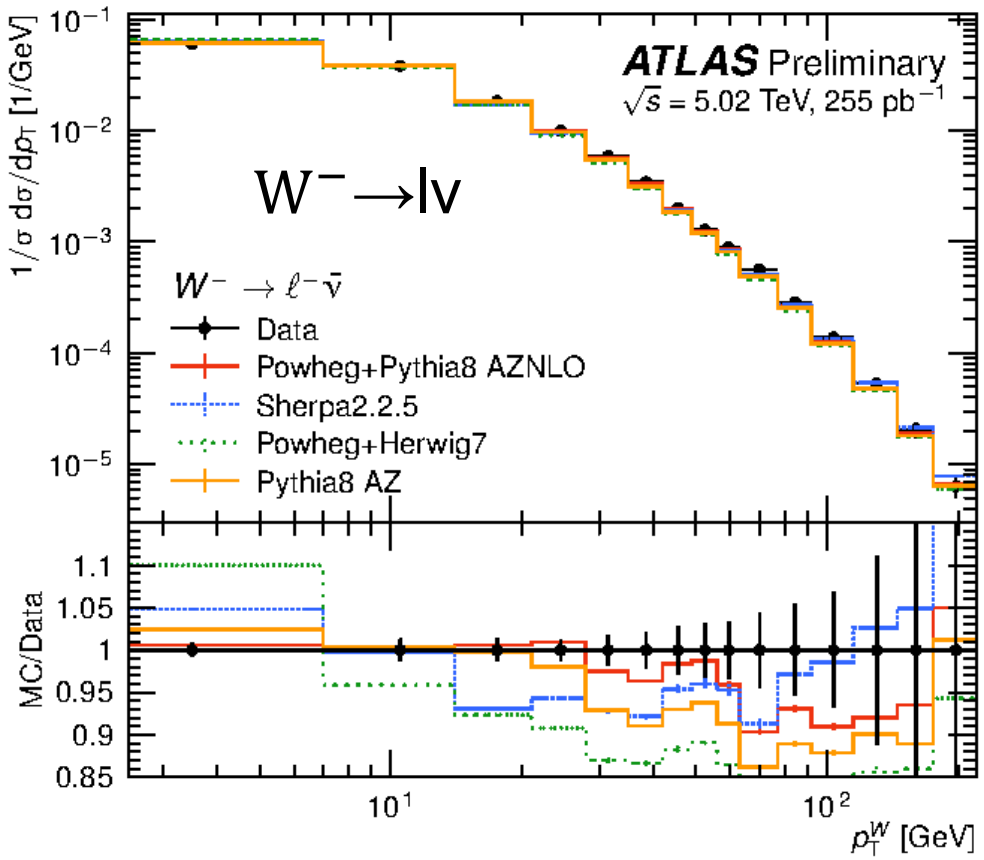

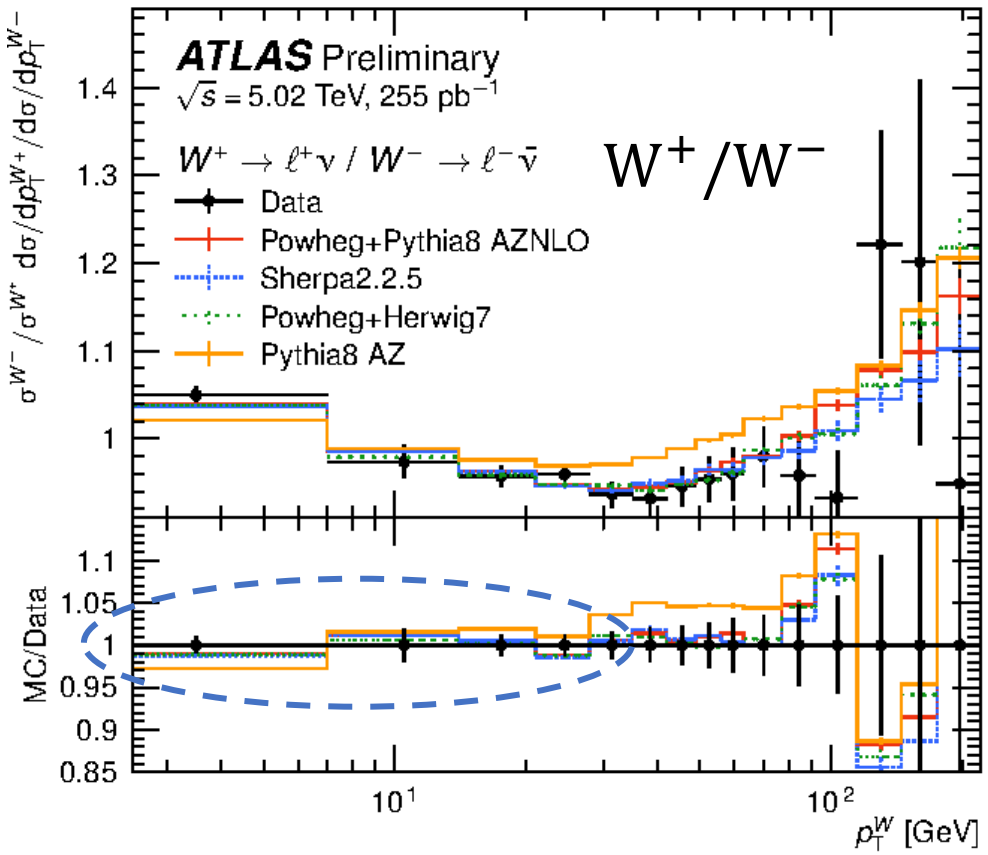

Measurement compared with various MC generators at 5.02 TeV.

- The differential cross-sections are valuable input to m_W measurement.
- Good data MC agreement for the W^+/W^- ratio.

p_T^W differential cross-section: 5.02 TeV

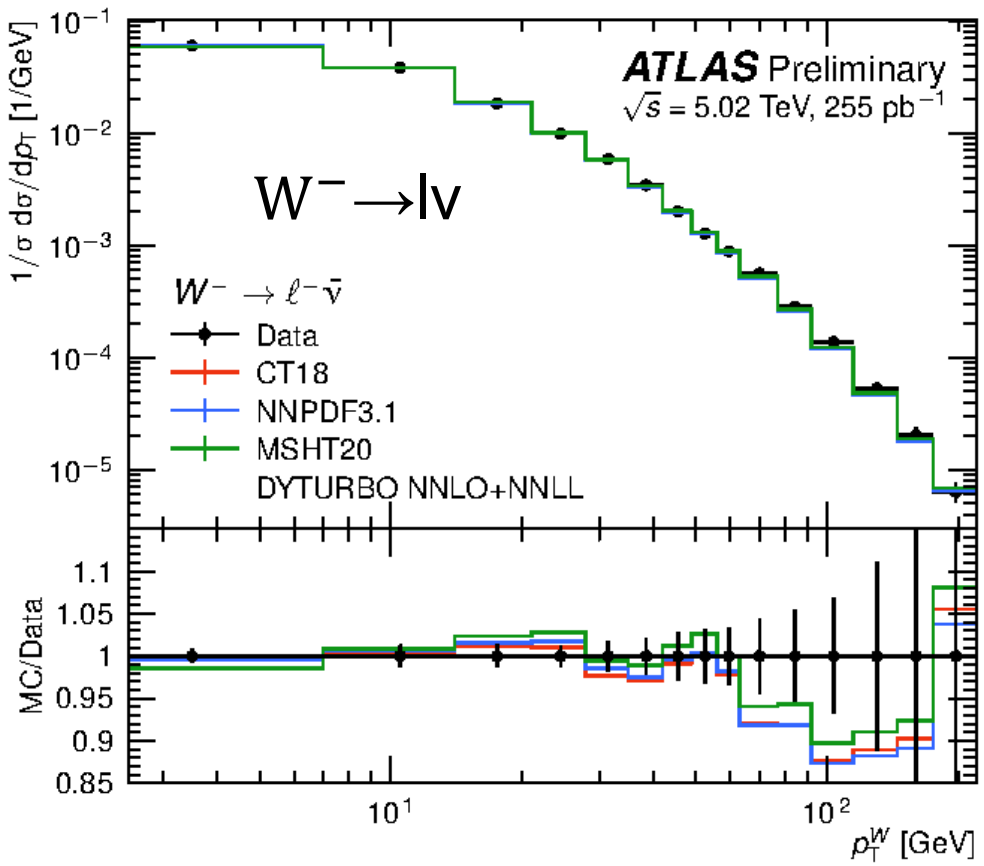

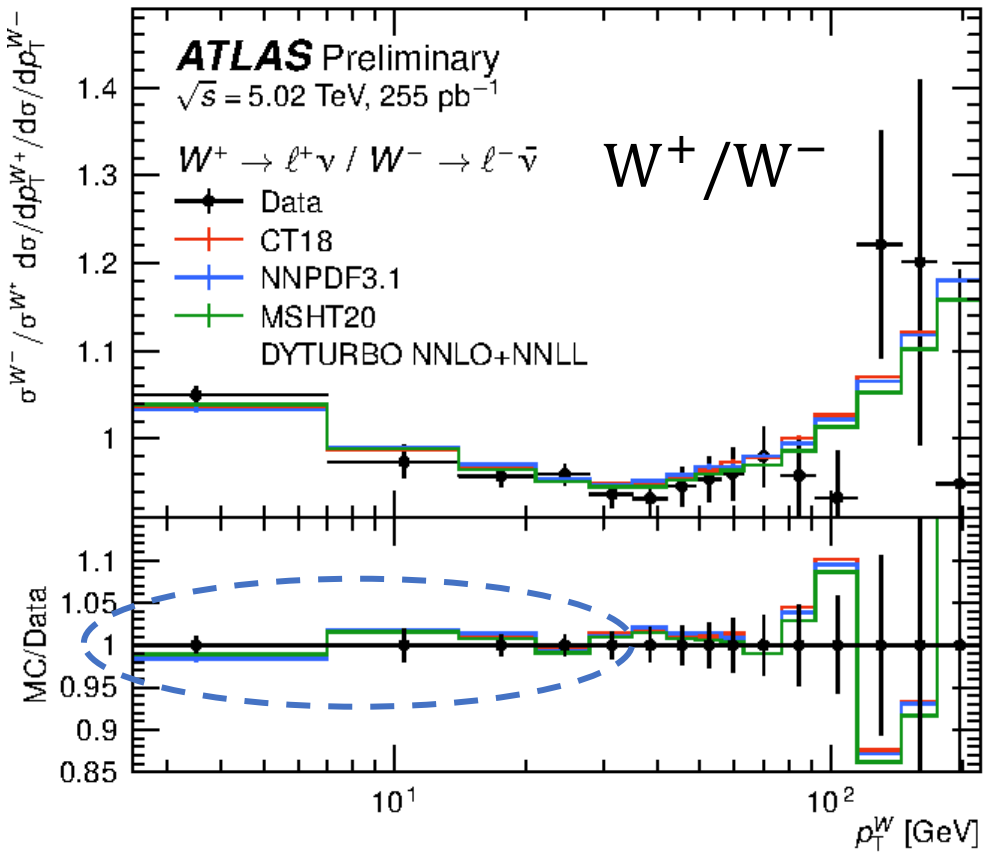

DYTURBO @NNLO+NNLL for pp -> W -> lv.

- The differential cross-sections are valuable input to m_W measurement.
- Good data MC agreement for the W^+/W^- ratio.

p_T^W differential cross-section: 13 TeV

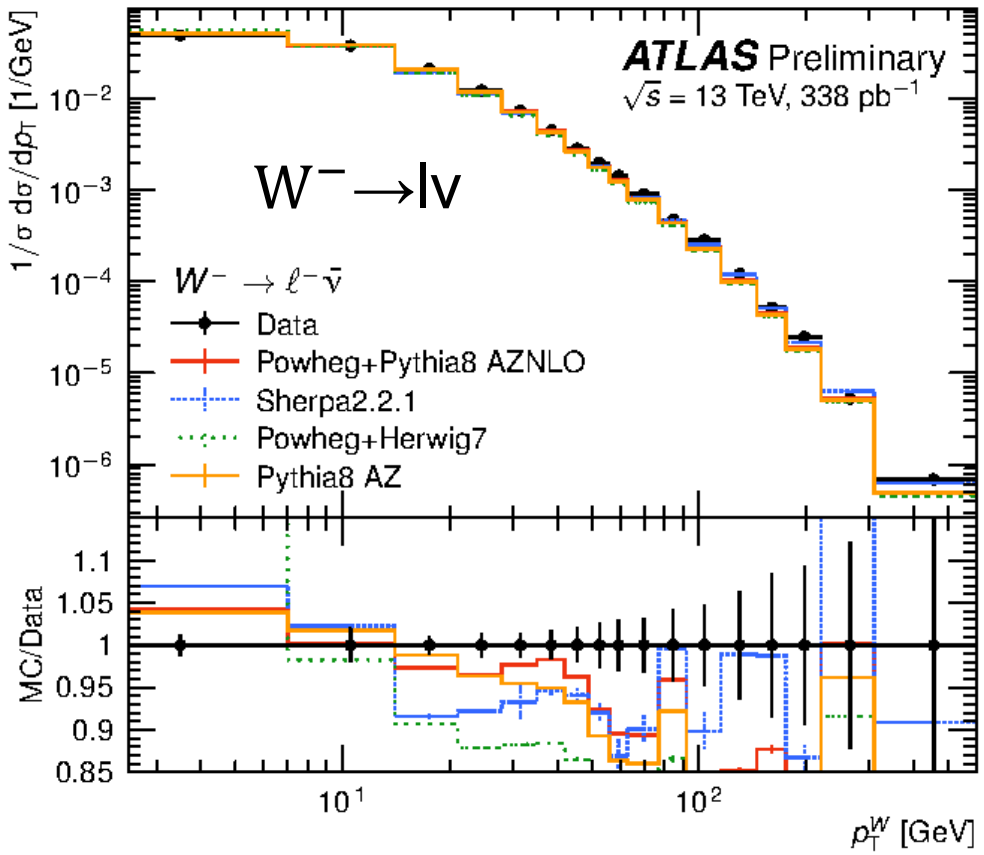

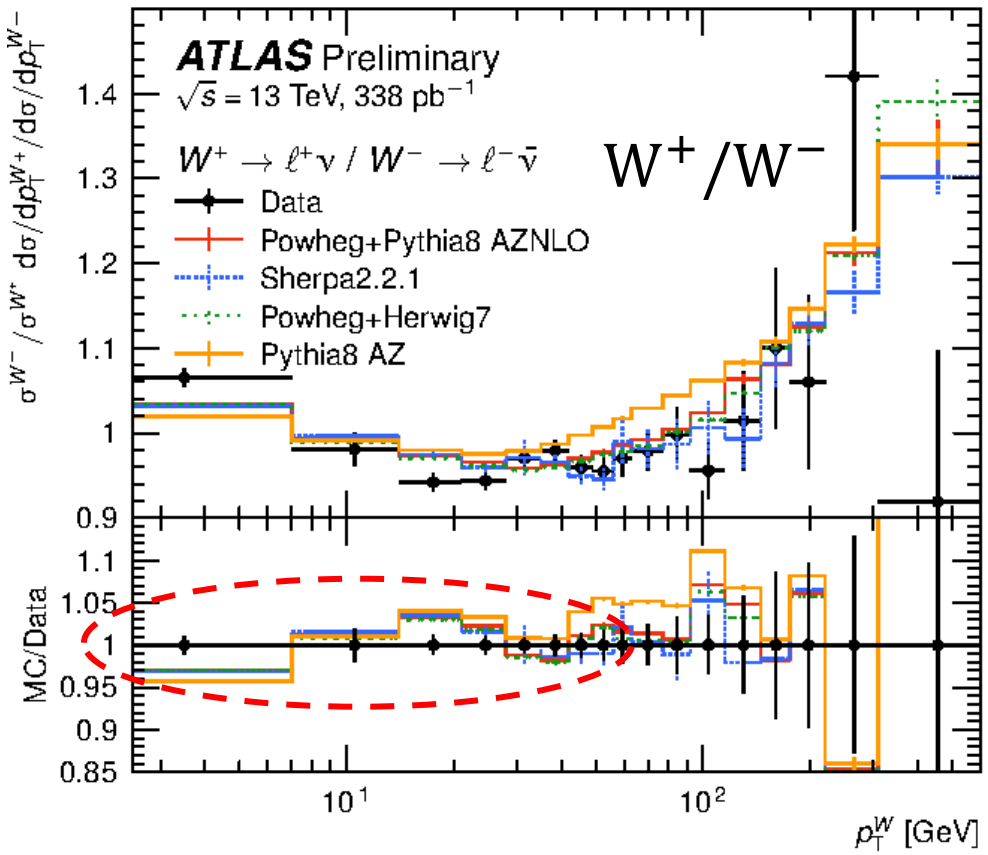

Measurement compared with various MC generators at 13 TeV.

- The differential cross-sections are valuable input to m_W measurement.
- Tension in the low p_T region of the W^+/W^- ratio.

p_T^W differential cross-section: 13 TeV

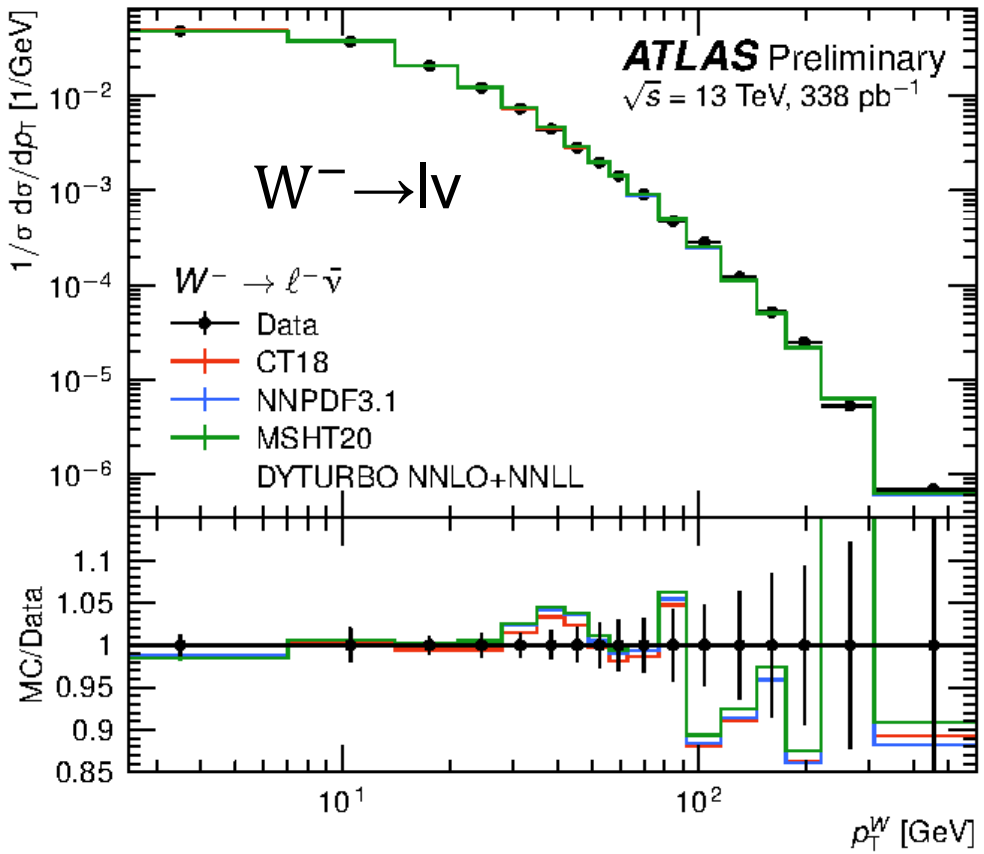

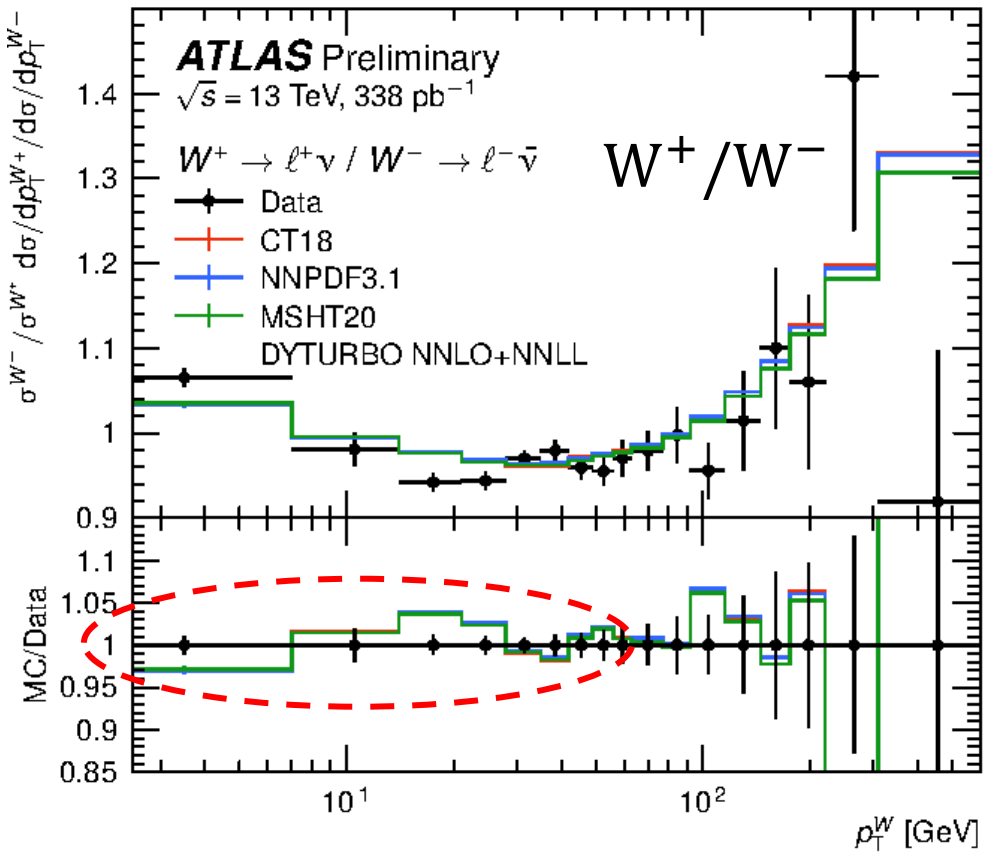

DYTURBO @NNLO+NNLL for pp -> W -> lv.

- The differential cross-sections are valuable input to m_W measurement.
- Tension in the low p_T region of the W^+/W^- ratio.

p_T^Z differential cross-section

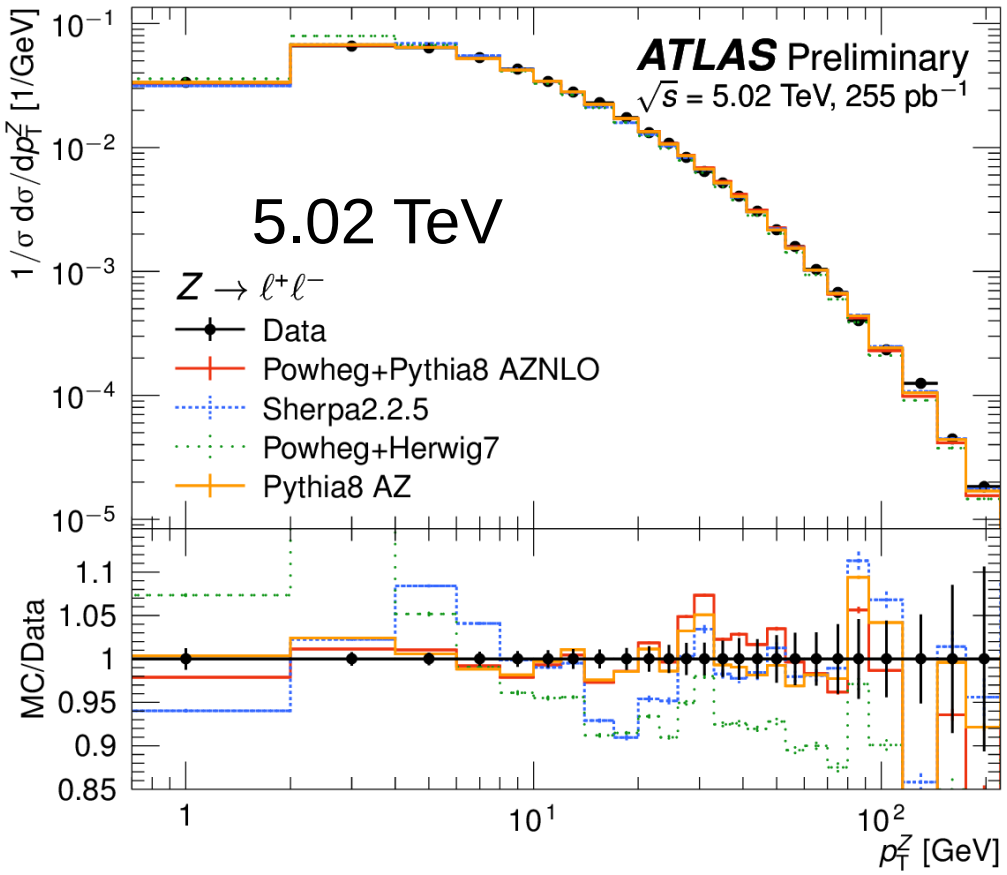

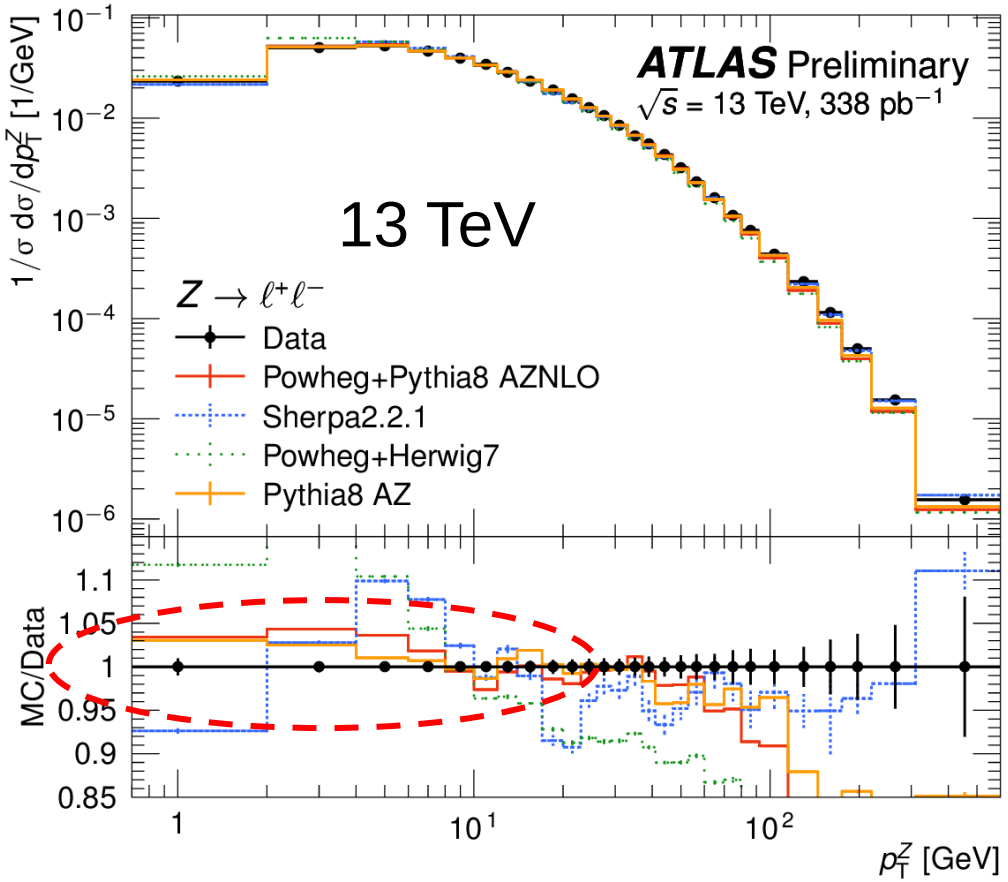

- The parton showers tuned using ATLAS 7 TeV data agrees with the measurement at 5.02 TeV.
- Some discrepancy in the low p_T region at 13 TeV.

p_T^W measurement: integrated cross-sections

Integrated fiducial cross-section

Process	Cross section at $\sqrt{s} = 5.02$ TeV [pb]	Cross section at $\sqrt{s} = 13$ TeV [pb]
$W^- \to \ell\nu$	1385 ± 2 (stat.) ± 5 (sys.) ± 15 (lumi.)	3486 ± 3 (stat.) ± 18 (sys.) ± 34 (lumi.)
$W^+ \to \ell\nu$	2228 ± 3 (stat.) ± 8 (sys.) ± 23 (lumi.)	4571 ± 3 (stat.) ± 21 (sys.) ± 44 (lumi.)
$Z \to \ell\ell$	333.0 ± 1.2 (stat.) ± 2.2 (sys.) ± 3.3 (lumi.)	780.3 ± 2.6 (stat.) ± 7.1 (sys.) ± 7.1 (lumi.)

- Sufficient statistics and small systematics.
- High precision luminosity calibration: 1% at 5.02 TeV & 0.92% at 13 TeV.
- One of the most accurate cross-section measurements at hadron colliders.

Integrated cross-section ratios

Processes	Cross-section ratio at 5.02 TeV	Cross-section ratio at $\sqrt{s} = 13$ TeV
W^+/W^-	1.611 ± 0.003 (stat.) ± 0.004 (sys.)	1.312 ± 0.001 (stat.) ± 0.003 (sys.)
W^-/Z	4.16 ± 0.01 (stat.) ± 0.05 (sys.)	4.46 ± 0.01 (stat.) ± 0.07 (sys.)
W^+/Z	6.69 ± 0.02 (stat.) ± 0.08 (sys.)	5.84 ± 0.01 (stat.) ± 0.09 (sys.)
$W^\pm/Z$	10.85 ± 0.04 (stat.) ± 0.11 (sys.)	10.31 ± 0.02 (stat.) ± 0.15 (sys.)

Z→ll: p_T^l > 25 GeV, $|\eta_l|$ < 2.5, and 66 < m_{ll} < 116 GeV

W→lν : p_T^l > 25 GeV, $|\eta_l|$ < 2.5, p_T^ν > 25 GeV, and m_T > 50 GeV

p_T^W measurement: integrated cross-sections

PDF set	$W^- \to \ell\nu$	$W^+ \to \ell\nu$	$Z \to \ell\ell$
Cross-section at 5.02 TeV [pb]			
CT18	1364	2199	320.9
MSHT20	1351	2185	324.3
NNPDF3.1	1381	2232	329.8
Data	1384 ± 16	2228 ± 25	333.0 ± 4.1
Cross-section at 13 TeV [pb]			
CT18	3410	4462	749.8
MSHT20	3397	4457	766.1
NNPDF3.1	3452	4513	771.4
Data	3486 ± 38	4571 ± 49	780.3 ± 10.4

Measured integrated fiducial cross-sections are compared with predictions of DYTURBO @NNLO+NNLL, using different PDF sets.

The best compatibility is found between data and NNPDF3.1

Z→ll: p_T^l > 25 GeV, $|\eta_l|$ < 2.5, and 66 < m_{ll} < 116 GeV
W→lν : p_T^l > 25 GeV, $|\eta_l|$ < 2.5, p_T^ν > 25 GeV, and m_T > 50 GeV

Conclusions

- The transverse momentum spectra of the W and Z bosons at 5.02 TeV and 13 TeV have been measured using ATLAS Run 2 low pile-up data.
- The dedicated datasets, reconstruction, calibration and data-driven multijet estimation render a granularity of 7 GeV in the low p_T^W region, with typically a 1~2% level precision.
- The measured p_T^W and p_T^Z differential cross-sections are compared with a variety of MC predictions, including the higher-order DYTURBO analytical resummation. All predictions show a small discrepancy with data for W^+/W^- at 13 TeV.
- The integrated cross-sections are reported with high precision. An improvement by a factor of ≥2 is found after the updated luminosity measurement.

Important input to the low pile-up m_W measurement!

Backup

MC samples and event selection

A MC 16 campaign was produced to match the low pile-up condition in data:

- W & Z production: Powheg+Pythia8 AZNLO, CT10 PDF
- Top-related background: Powheg+Pythia8
- Di-boson background: Sherpa
- Minimum-bias events: Pythia8 A3 tune with NNPDF2.3LO

Cut	Description
OSSF dilepton	Electron pair or muon pair
At least one lepton triggers the event	• Electron, $E_T > 15\ \mathrm{GeV}$, loose ID. • Or muon, $E_T > 14\ \mathrm{GeV}$.
Isolation	Ptcone20 / Min(p_T^l, 50GeV) < 0.1
Additional lepton veto	Veto >=3 muons (electrons) with p_T^l> 20 GeV + medium (loose) ID
Kinematics	$66 < m_{ll} < 116\ \mathrm{GeV}$

Analysis cuts for Z signal selection

Electron SF and calibration

- The electron reconstruction SF: extrapolation of the standard high-mu SFs to the low-mu regime applied to both the 5.02 and 13 TeV datasets.
- The identification SF: measured in-situ separately for the 5.02 and 13 TeV data.
- Isolation and trigger efficiencies SF: measured in-situ using the 5.02 and 13 TeV combined datasets.

- Electron energy scale and resolution corrections are measured in-situ using Z->ee events from the low-mu dataset.

Muon SF and calibration

- Muon reconstruction efficiencies: extrapolated from high-mu measurements.
- The muon trigger, isolation and TTVA efficiencies: measured in-situ.

- Momentum scale and resolution: derived from the high-mu data.
- Sagitta bias corrections: derived from 2017 low-mu datasets.

Iterative Bayesian unfolding

- Assuming the true distribution after the fiducial cut is T_j :

$$D_i = \sum_j M_{ij} \varepsilon_j T_j + B_i$$

- Then the unfolded spectrum $\widehat{U}_j$ estimates the underlying T_j :

$$\widehat{U}_j = \sum_i U_{ij} (D_i - B_i) \times p_i$$

i = reco-level bin, j = unfolded-level bin

M_{ij}: Migration matrix

ε_j: Reconstruction efficiency

p_i: Reconstruction purity

U_{ij}: The unfolding transformation

References:
[1] doi.org/10.1016/0168-9002(95)00274-X
[2] arxiv.org/abs/1010.0632

Uncertainty propagation

- **Data statistics** $\widetilde{U}_j^{\alpha} = \sum_i U_{ij}(D_i^{\alpha} - B_i)$

Fluctuate the data -> calculate the spread at unfolded level.

- **MC statistics** $\widetilde{U}_j^{\alpha} = \sum_i U_{ij}^{\alpha}(D_i - B_i)$

Fluctuate the migration matrix, efficiency and purity corrections -> calculate the spread at unfolded level.

- **Experimental** systematics $\widetilde{U}_j^{\alpha} = \sum_i U_{ij}^{\alpha}(D_i - B_i)$

Vary the migration matrix, efficiency and purity corrections.

- **Background** systematics $\widetilde{U}_j^{\alpha} = \sum_i U_{ij}(D_i - B_i^{\alpha})$

Vary the estimation of background.

p_T^V reweighting

- For a first fit, the data/MC agreement is optimized at reco-level by reweighting the truth-level p_T^V distribution. Once the reweighting function is determined, it will be used to correct the p_T^V distribution in the MC.
- A second fit is performed after p_T^V reweighting as a closure test. The uncertainties in the fit parameters are propagated to the unfolding.

Optimization of reco-level distribution.

$$\chi^2 = \sum_{ij} \Delta_i^T C_{ij}^{-1} \Delta_j ,$$

$$\Delta_i = (D_i - B_i) - \sum_j R_{ij} \times (w_T(p_T^W))_j$$

i: reco-level bin
j: truth level bin

$$(w_T(p_T^W))_j = N_j \left[\left(1 + a\, p_{T,j}^W + b\, {p_{T,j}^W}^2\right) * \left(1 - c + c * r_{\mathrm{NNPDF/CT10}}(p_{T,j}^W)\right) \right]$$

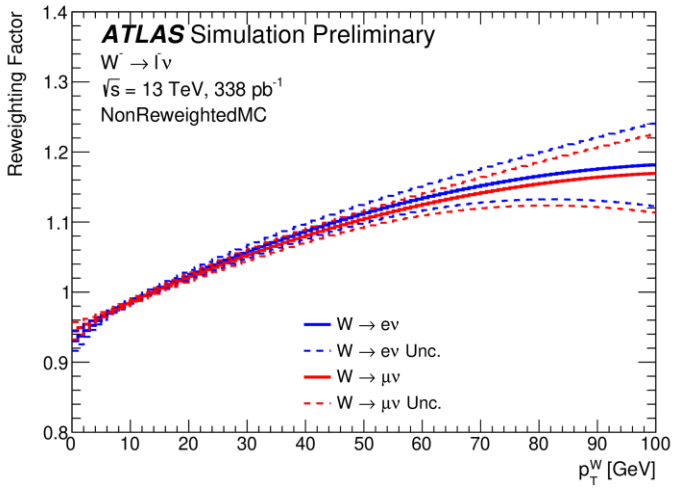

Fitted truth reweighting functions of p_T^W. The final choice is the eμ average.

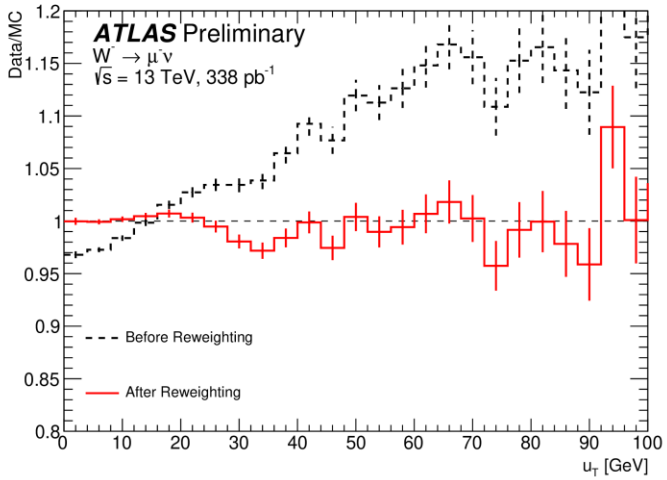

Data/MC ratio for reco-level u_T in 13 TeV $W^- \rightarrow \mu\nu$ channel, before and after the p_T^V modelling correction.

Unfolding bias uncertainty for p_T^W

- Fit uncertainty: uncertainties in the parameters of the p_T^W reweighting function.

- Parametrization uncertainty: the difference caused by determining the p_T^W reweighting using an alternative function.

- Initial (p_T^W, y) uncertainty: reweight (p_T^W, y) to alternative MC predictions to get different initial spectra.

- The non-closure of the reweighting.

The measurement of the p_T^Z spectrum

- $p_T^Z(p_T^{ll})$ - $p_T^Z(u_T)$ compatibility and uncertainty break-down

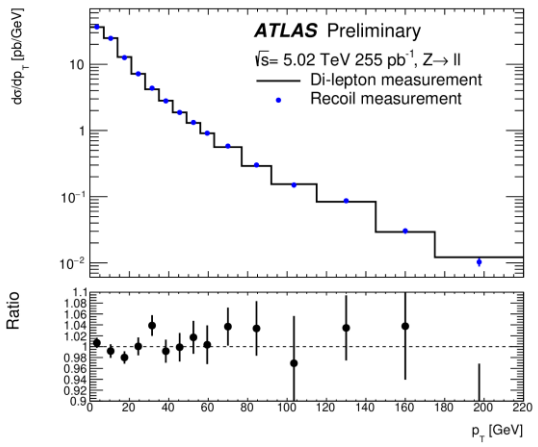

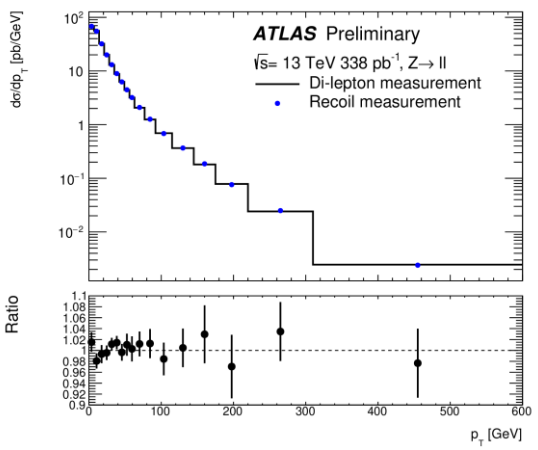

χ^2	5.02 TeV	13 TeV
Stat. + Syst.	14.9 / 14	8.7 / 16
p-value	38.5%	85%

$p_T^Z(p_T^{ll})$ - $p_T^Z(u_T)$ compatibility test at 5.02 TeV (left) and at 13 TeV (right).
Good compatibility is found at both center-of-mass energies.

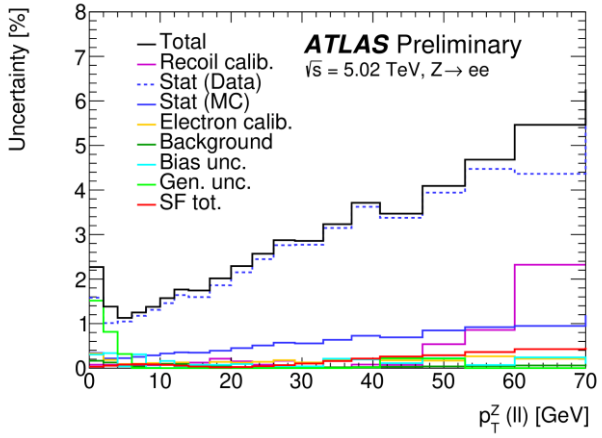

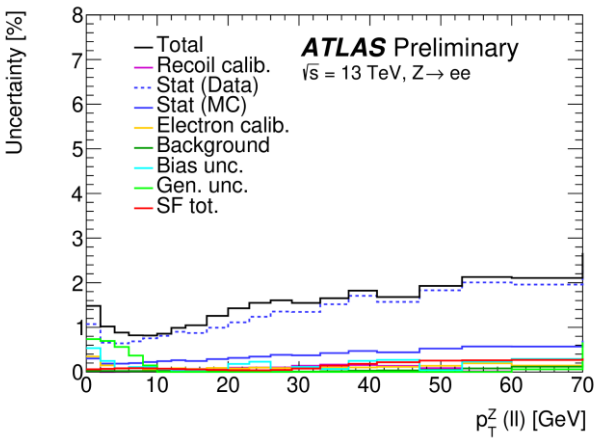

Break-down of unfolded-level shape uncertainties for p_T^{ee} at 5.02 TeV (left) and at 13 TeV (right).

The data statistics dominates the uncertainty.

The unfolding bias and the optimization of unfolding for p_T^Z follow the methods described for p_T^W.

p_T^Z differential cross-section

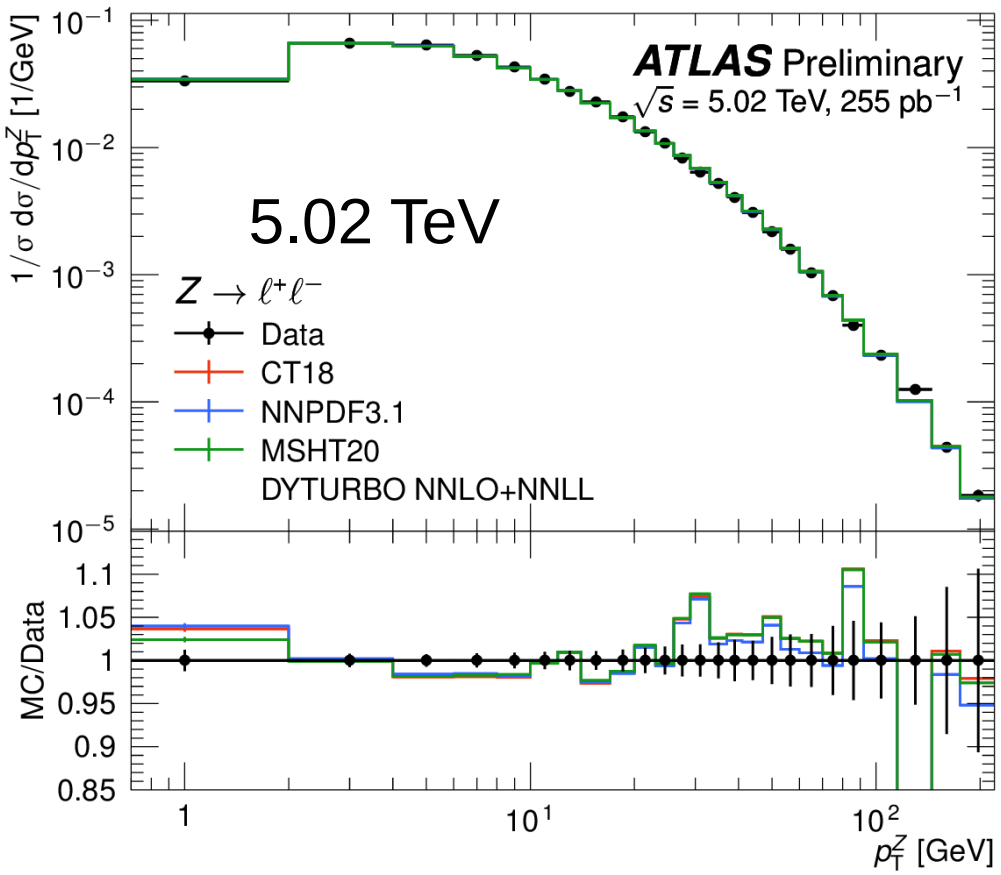

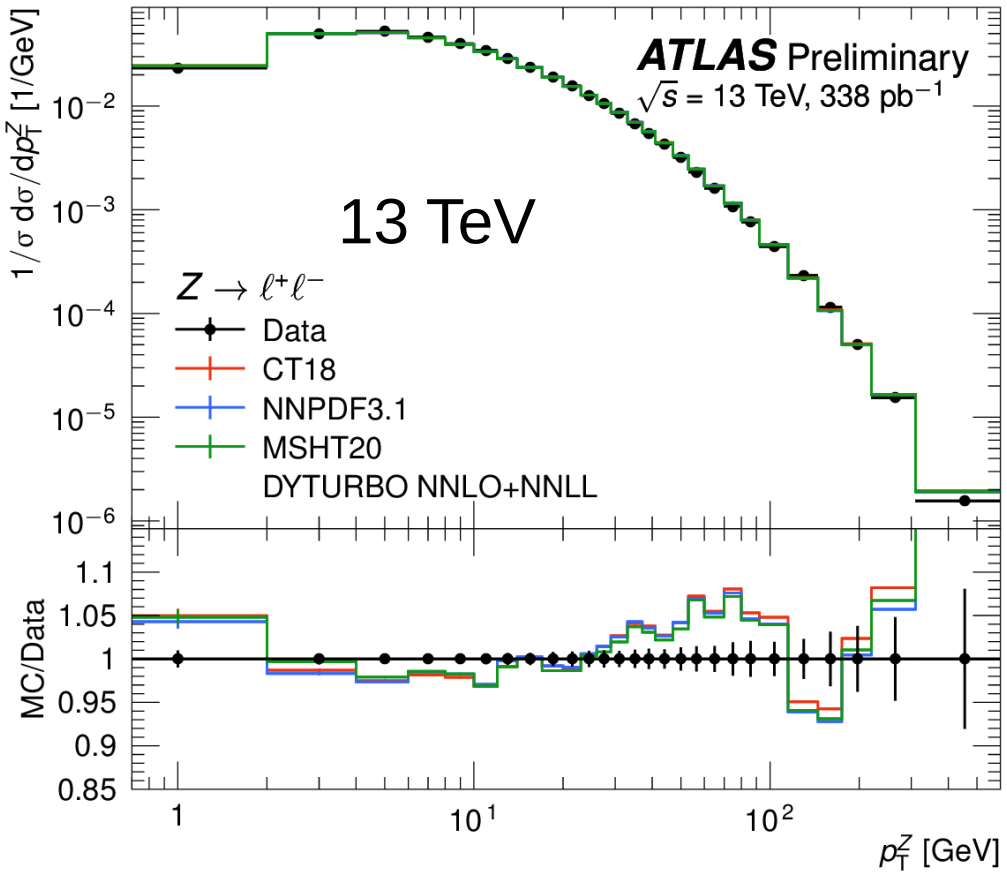

Measured p_T^Z spectra vs NNLO+NNLL DYTURBO predictions using different PDF sets.

W/Z ratios

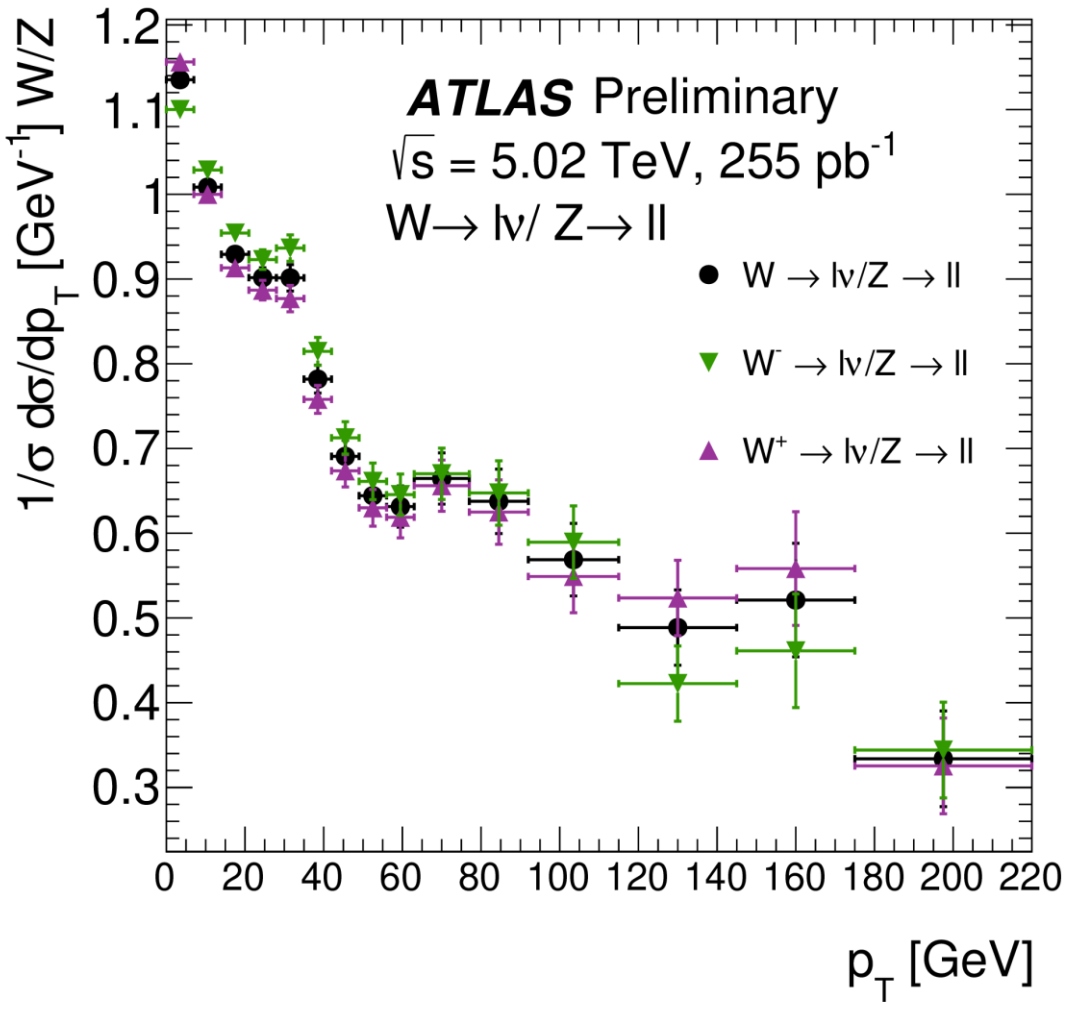
ATLAS Preliminary
√s = 5.02 TeV, 255 pb-1
W→ lν/ Z→ ll
W → lν/Z → ll
W- → lν/Z → ll
W+ → lν/Z → ll
1/σ dσ/dpT [GeV-1] W/Z
pT [GeV]

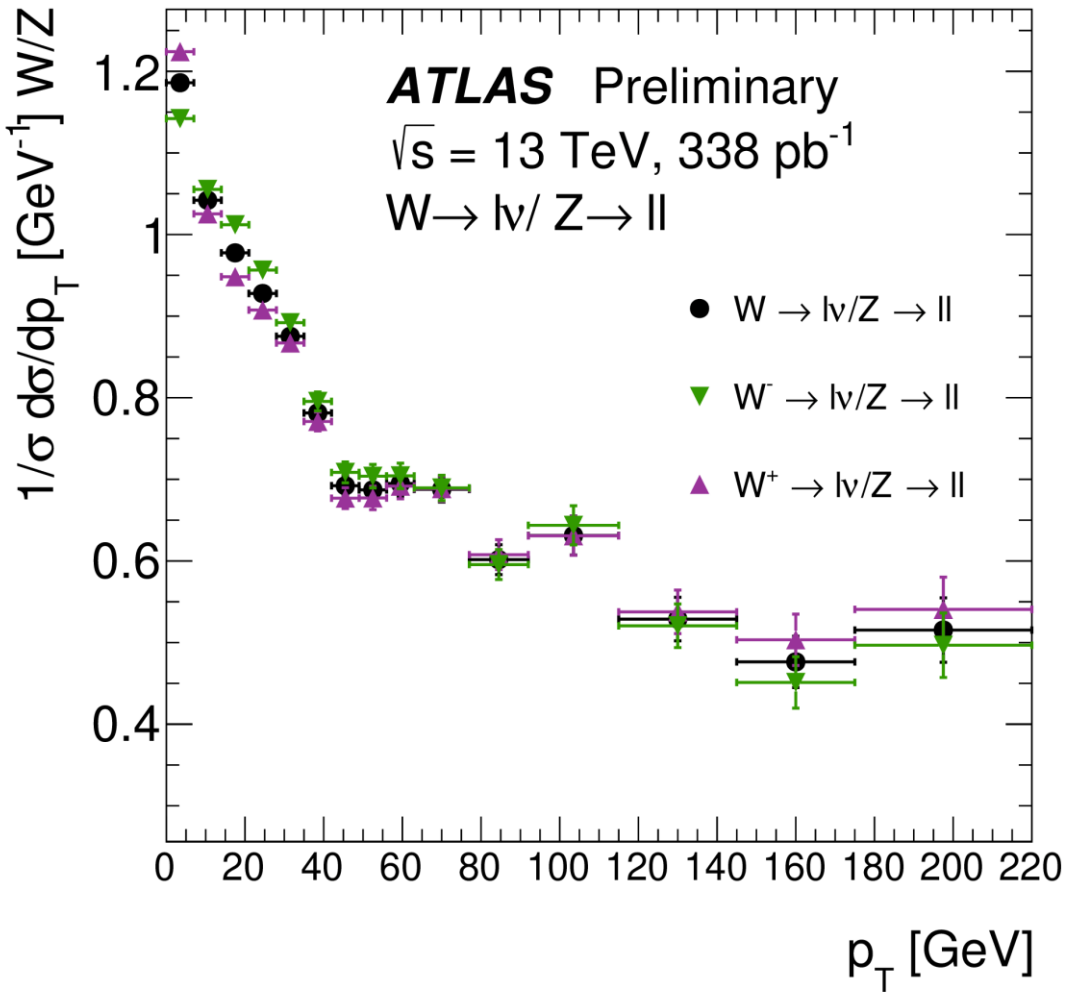
ATLAS Preliminary
√s = 13 TeV, 338 pb-1
W→ lν/ Z→ ll
W → lν/Z → ll
W- → lν/Z → ll
W+ → lν/Z → ll
1/σ dσ/dpT [GeV-1] W/Z
pT [GeV]

MJ yield

Channel	$W^- \to e^-\nu$	$W^+ \to e^+\nu$	$W^- \to \mu^-\nu$	$W^+ \to \mu^+\nu$
	5.02 TeV $W \to \ell\nu$			
MJ background yield	2200	2300	300	500
Statistics	300 (14%)	340 (14%)	120 (40%)	140 (25%)
Extrapolation	290 (13%)	340 (15%)	210 (70%)	230 (40%)
u_T-dependence	600 (29%)	800 (40%)	270 (90%)	300 (50%)
Total uncertainty	700 (32%)	900 (40%)	340 (110%)	400 (70%)
	13 TeV $W \to \ell\nu$			
MJ background yield	27000	29000	6000	6000
Statistics	800 (3.0%)	900 (3.0%)	310 (5%)	330 (5%)
Extrapolation	2400 (9%)	2400 (8%)	1400 (25%)	1500 (23%)
u_T-dependence	4200 (15%)	4300 (15%)	1400 (24%)	1400 (21%)
Total uncertainty	5000 (18%)	5000 (17%)	2000 (34%)	2000 (31%)

Channel	$Z \to ee$	$Z \to \mu\mu$
	5.02 TeV $Z \to \ell\ell$	
MJ background yield	0^{+100}_{-0}	16 ± 8
	13 TeV $Z \to \ell\ell$	
MJ background yield	110 ± 70	180 ± 40